Update of cBPM results and plans for cryomodule tests

Laura Karina Pedraza,
A. Aryshev, B. Gimeno-Martínez, C. Blanch-Gutierrez, D. Esperante-Pereira, D. Gonzáles-Iglesias, J.C. Fernández-Ortega, M. Boronat, M. Moreno-Llácer, N. Fuster-Martínez, N. Terunuma, T. Okugi

Cold BPM R&D meeting, 06/10/2026

laura.pedraza@ific.uv.es

Update of cBPM results and plans for cryomodule tests

Cold BPM R&D meeting
06/10/2026

INSTITUT DE FÍSICA CORPUSCULAR

Introduction

I. Summary of ATF measurements with BPM
   A) Setup and methodology
   B) Main results
   C) System limitations and alternatives

II. Cryomodule test setup and preparation
   A) Installation and measurement
   B) Preparation for measurements
   C) Calibration

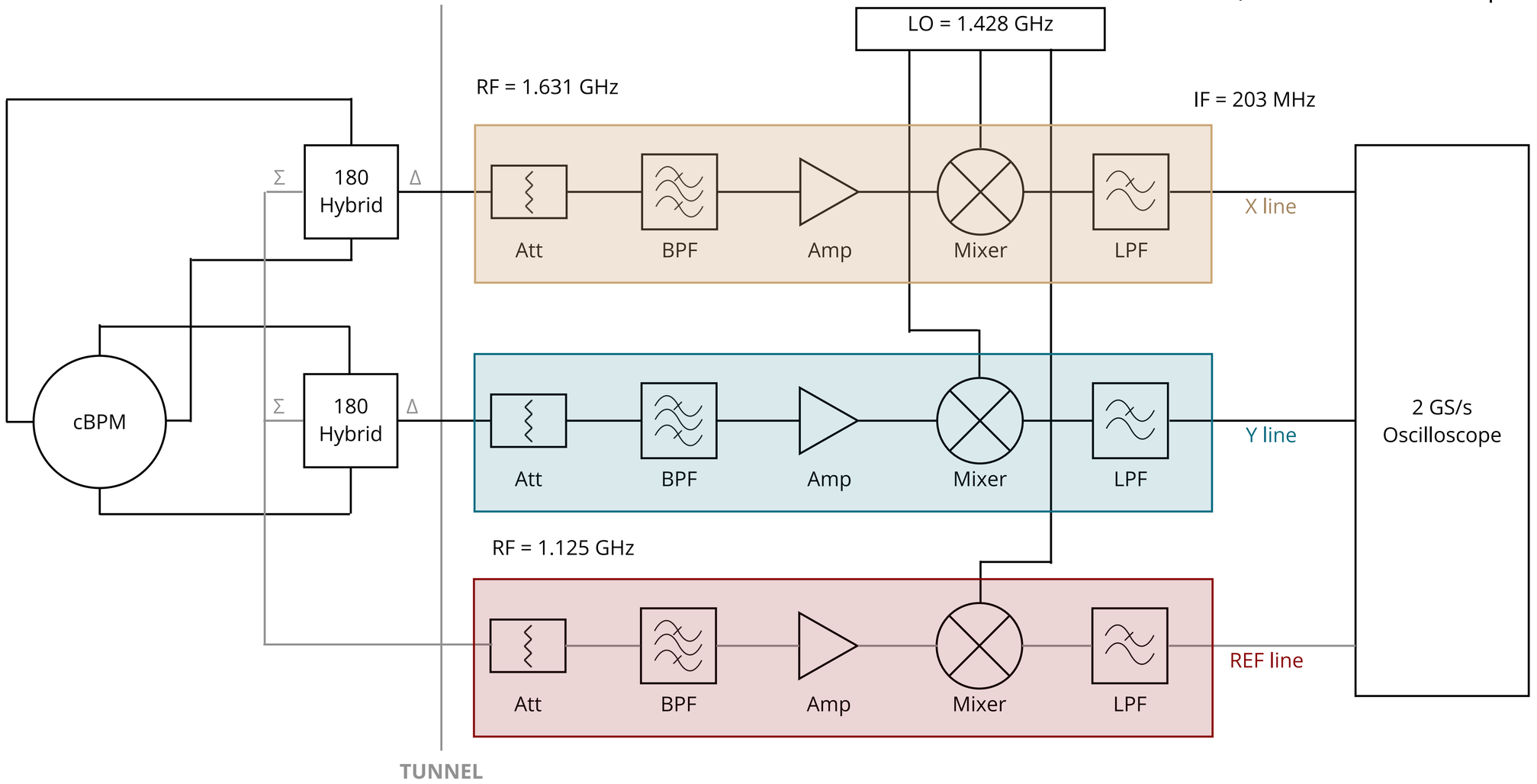
III. Measurements planning
   A) First week
   B) Second week
   C) Third week
   D) Fourth and fifth week

Conclusion

I. Summary of ATF measurements with BPM

A) Setup and methodology

3 identical lines of down-conversion to ~200 MHz:
-two for x and y signals (with RF = 1.631 GHz).
-one for reference signal (with RF = 1.125 GHz)
(the tail of the monopole mode is taken).



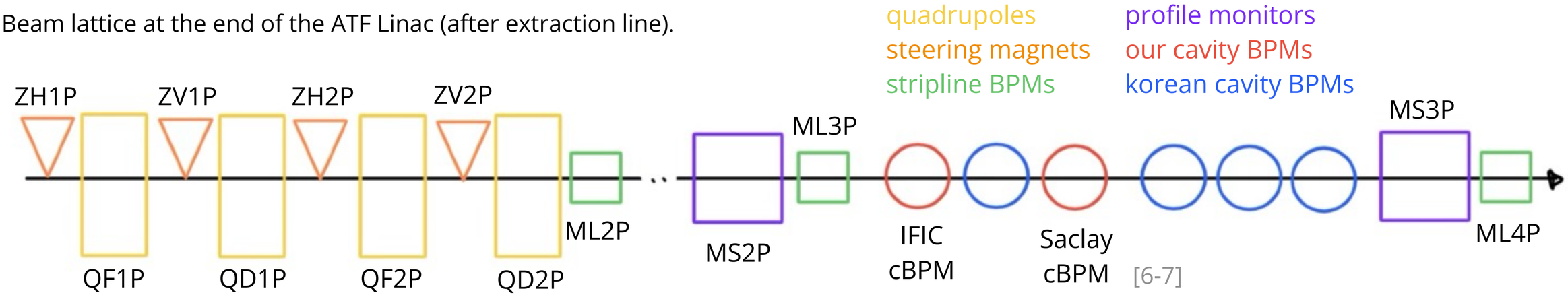
Reference signal is taken from the same BPM and the same LO is used for the 3 signals.

A digital down-conversion (DDC) algorithm is employed to extract the amplitude and phase of both signals.

I. Summary of ATF measurements with BPM

A) Setup and methodology

Beam lattice at the end of the ATF Linac (after extraction line).



Calibration:

The horizontal and vertical steering magnets (ZH2P and ZV2P) were used to induce a range of beam offsets in the X and Y planes for calibration.

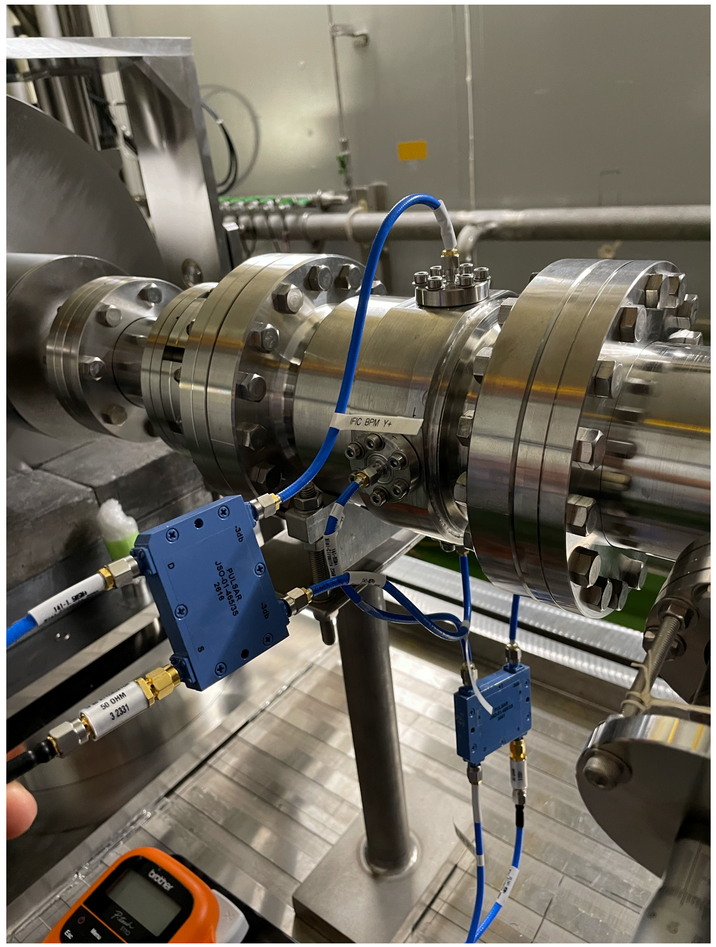
The cBPM measurements were converted to estimated beam positions using linear interpolation of stripline BPM readings from ML3P and ML4P, along with upstream and downstream profile monitors (MS2P and MS3P).

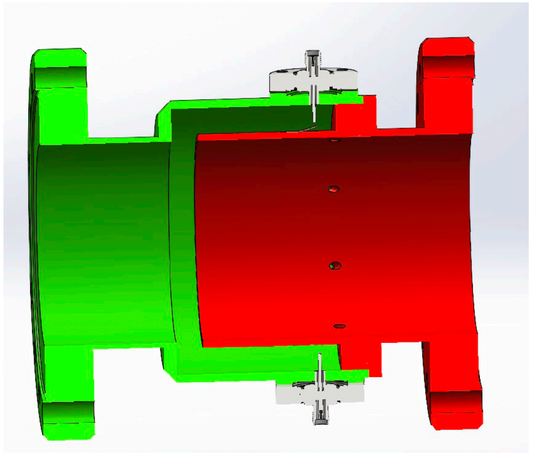
Resolution:

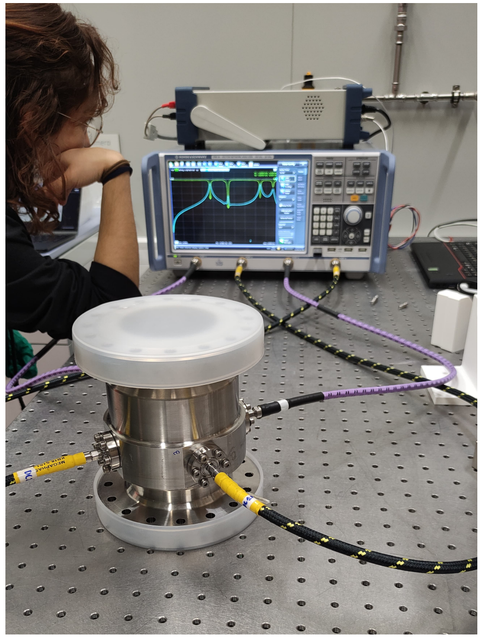
A set of P = 1000 pulses was acquired at a fixed beam position, and simultaneous measurements from 19 stripline BPMs and the CEA-Saclay cBPM were used to remove coherent beam motion, and evaluate the system noise.

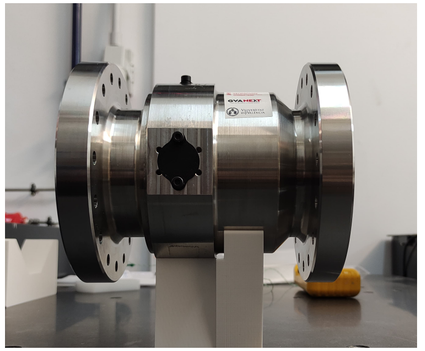
I. Summary of ATF measurements with BPM

B) Main results









- Designed, built and tested a 1.631 GHz re-entrant cBPM using commercial stainless steel feedthroughs suitable for cryogenic operation.
- System achieved **~2.98 µm Y-axis resolution** (at 0.74 nC/bunch) with a 2 mm linear dynamic range (compared with achieved 3.58 µm that was obtained with Saclay cBPM)
- A cryogenic test will be carried out in collaboration with STF (KEK) to further validate the new prototype.

I. Summary of ATF measurements with BPM

C) System limitations and alternatives

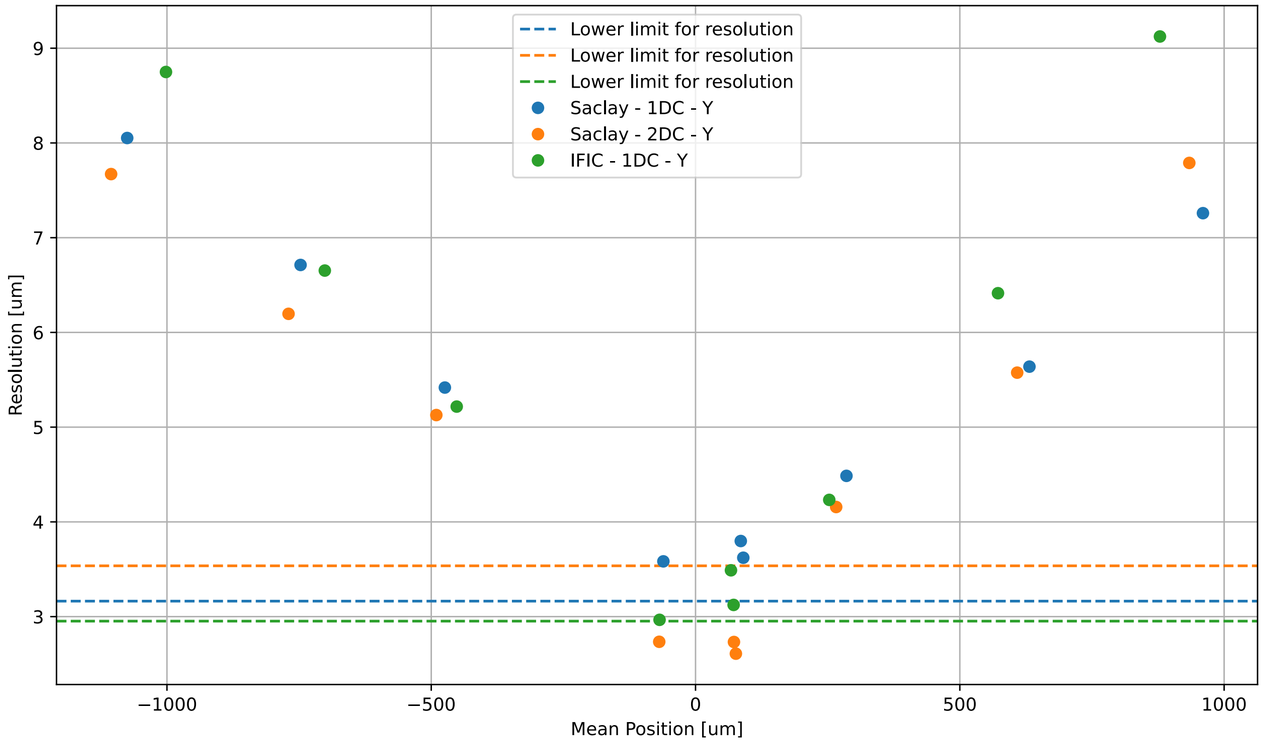
➡ **Current stripline BPMs resolution limits the measurements:** higher-precision monitors are needed to prove sub-micron capability for future colliders.

Influence of stripline BPMs resolution and correlation coefficient errors on the resolution estimation:

We performed numerical pseudo-experiments to asses an estimated lower limit resolution:

Table 2: Resolution error contributions breakdown from pseudo-experiments method (in μm).

	Meas. res	Resolution error		
	σ	$\sigma_{err,BPMs}$	$\sigma_{err,v}$	σ_{err}
Striplines only	**4.17**	3.30	0.78	3.44
with Saclay cBPM	**2.98**	2.34	0.59	2.46



➡ **Alternatives:**
Building one (or two) additional BPMs to test the resolution properly in ATF (independently of the stripline BPM data)
Installing the BPM in another accelerator (that has cBPMs) and perform the test in a different facility (CLEAR or DESY)

Update of cBPM results and plans for cryomodule tests

Cold BPM R&D meeting
06/10/2026

INSTITUT DE FÍSICA CORPUSCULAR

Introduction

I. Summary of ATF measurements with BPM
   A) Setup and methodology
   B) Main results
   C) System limitations and alternatives

II. Cryomodule test setup and preparation
   A) Installation and measurement
   B) Preparation for measurements
   C) Calibration

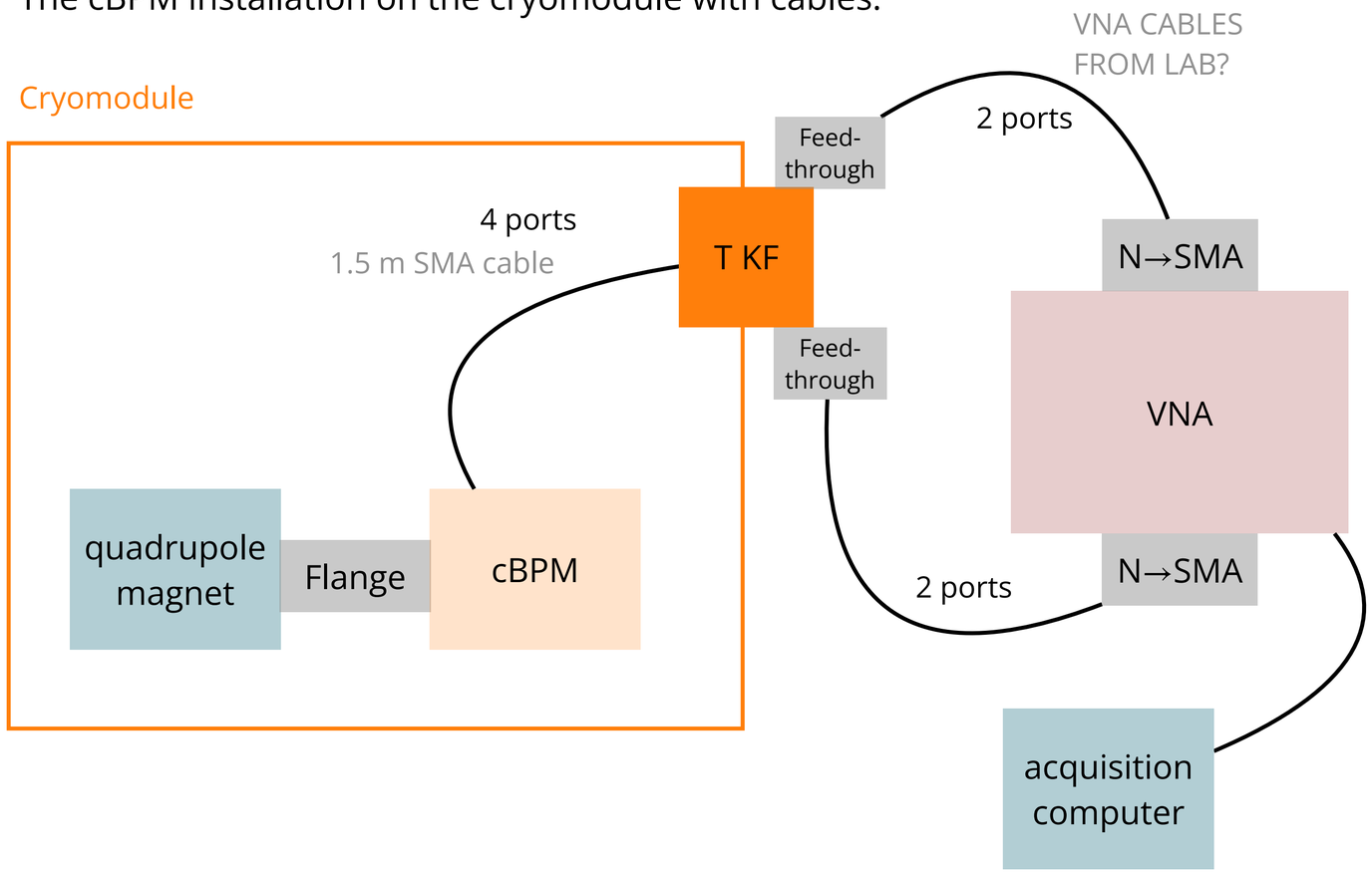
III. Measurements planning
   A) First week
   B) Second week
   C) Third week
   D) Fourth and fifth week

Conclusion

II. Cryomodule test setup and preparation

A) Installation and measurement

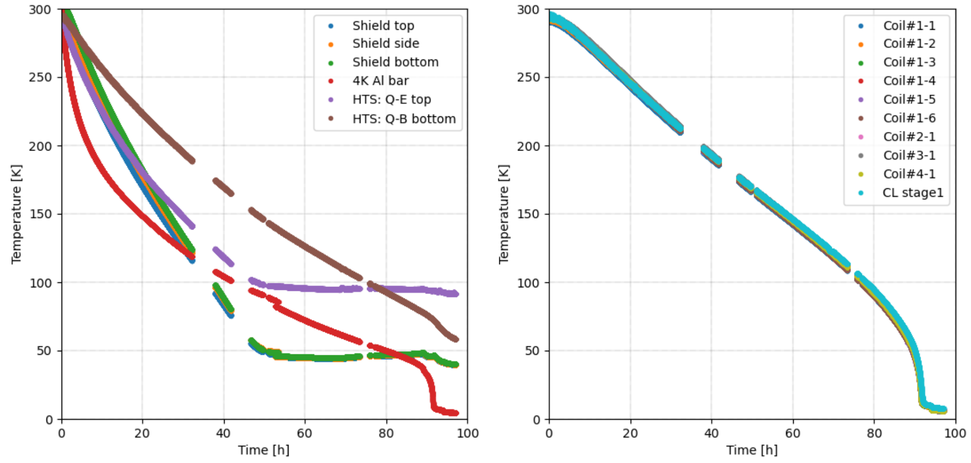
The cBPM installation on the cryomodule with cables:



Description of measurement:

Acquisition of Scattering parameters *.s4p VNA data every 15 minutes (?) to monitor changes in cBPM RF parameters as a function of time/temperature during cooling down to cryogenic temperatures (4 K).

Source: Tomohiro Yamada



II. Cryomodule test setup and preparation

B) Preparation for measurements

Preliminary considerations:

- The VNA has to be calibrated with calibration unit at the cBPM place and with cables installed on the cryomodule
- The cBPM + flanges weight approximately 10 kg, so the cooling down time to 4 K can be up to 5 days
- After cooling, the warming up to room temperature process takes approximately 3 days. Take into account when planning measurements
- The vacuum process takes 1 night. Take into account when planning measurements
- The flange has to go through ultra-sonic cleaning before installation
- A computer has to be prepared with Python to perform the continuous measurements

Additional variables:

❖ **Temperature:**

- Monitor the temperature inside the cryomodule
  - Two sensors (available from KEK) can be placed in the BPM body
  - Monitor is accessible through LabView
  - Include Tº acquisition on VNA measurement code
- Monitor the temperature outside the cryomodule
  - Temperature on the building is very variable (+/- 10º)
  - Prepare an additional sensor to monitor the Tº changes outside the cryomodule
  - Include Tº acquisition on VNA measurement code

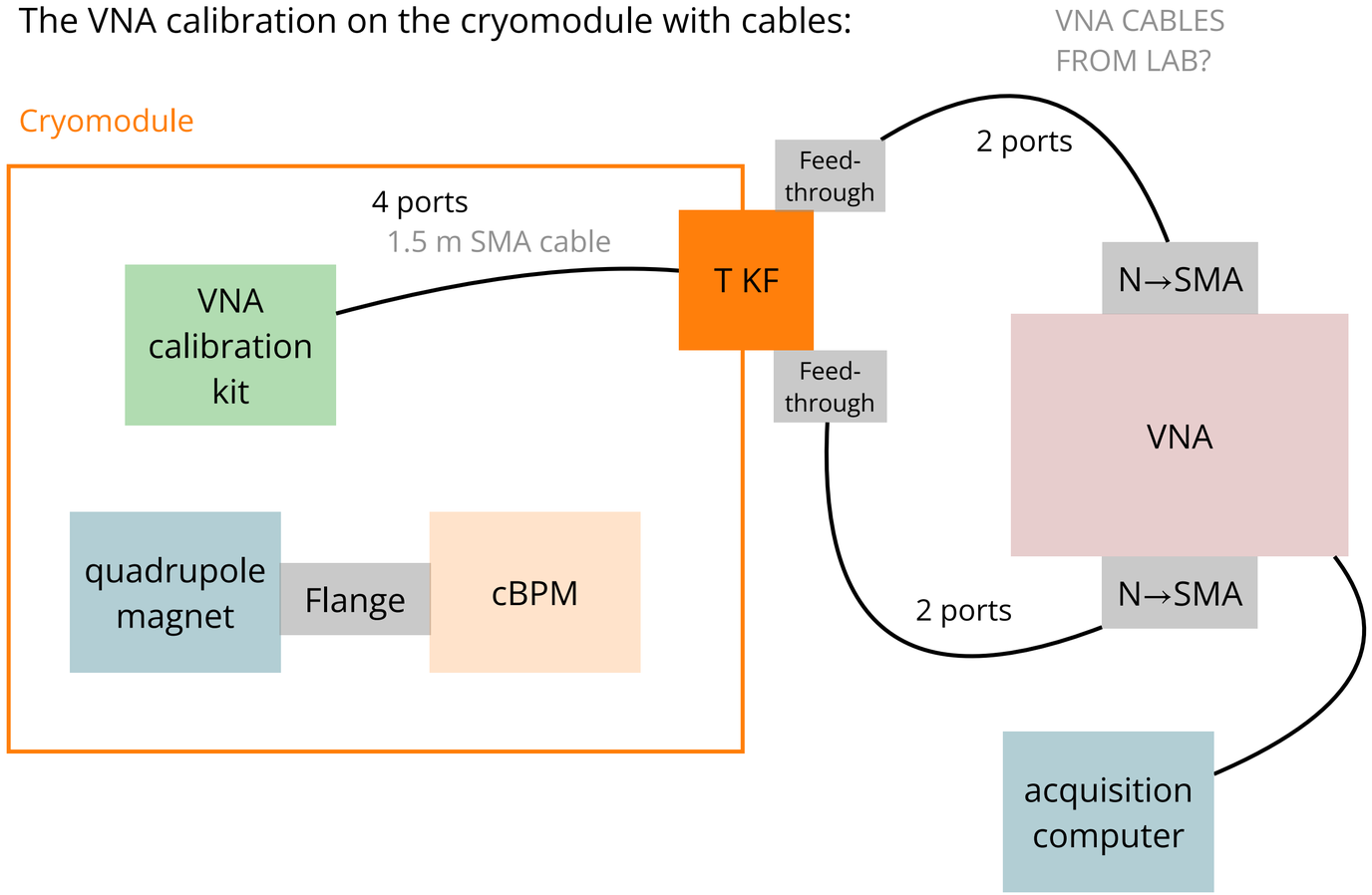
❖ **Quadrupole magnet current influence?**

- Possibility to turn on the current on the splitting quadrupole to check for possible effects on the cBPM

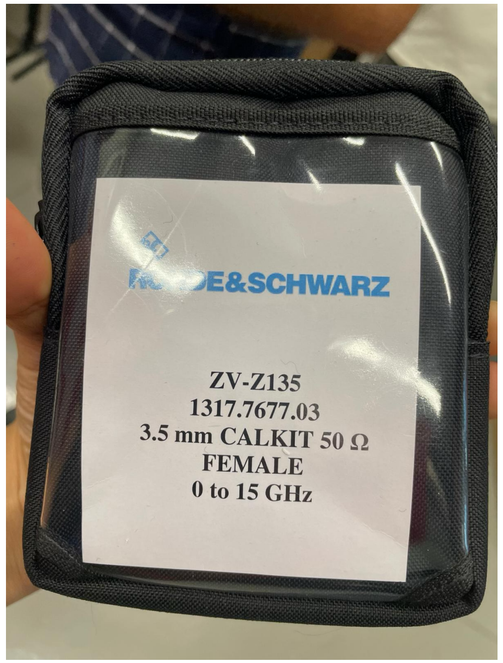
II. Cryomodule test setup and preparation

C) Calibration

The VNA calibration on the cryomodule with cables:



Calibration kit:



Compatibility?

It is necessary to import or manually enter the calibration kit definition parameter.

These definitions can be downloaded from the Rohde & Schwarz website (usually provided as an .s1p or .cal) and loaded via Cal → Cal Kit → Modify Cal Kit / Import on the E5071C VNA

Update of cBPM results and plans for cryomodule tests

Cold BPM R&D meeting
06/10/2026

INSTITUT DE FÍSICA CORPUSCULAR

Introduction

I. Summary of ATF measurements with BPM
   A) Setup and methodology
   B) Main results
   C) System limitations and alternatives

II. Cryomodule test setup and preparation
   A) Installation and measurement
   B) Preparation for measurements
   C) Calibration

III. Measurements planning
   A) First week
   B) Second week
   C) Third week
   D) Fourth and fifth week

Conclusion

III. Measurements planning

Calendar planning of the measurements:

NOVEMBER 2026

Sun	Mon	Tue	Wed	Thu	Fri	Sat
1	2	3	4	5	6	7
8	9	10	11	12	13	14
15	16	17	18	19	20	21
22	23	24	25	26	27	28
29	30	1	2			

First week:

Deinstallation of cBPM from ATF.

Installation on cryomodule.

- Verification of connection with VNA
- Cleaning of the flange
- Verification of connection with T° sensors

Second week:

LCWS26 + Preliminary tests and beginning test 1.

- Perform a preliminary test without cooling down to check stability of acquisition over time (1-2 days)
- Launch first cryogenic test before the weekend (5 days)

Third week:

End test # 1 and warming up

- Finish test # 1 and verification of result
- Start warming up to room temperature (3 days)

Forth and fifth week:

Perform test #2 and then deinstallation of the cBPM

- Start and monitor test # 2
- Finish test # 2 and verification of the result.
- Start warming up to room temperature (3 days).
- Deinstall cBPM



VNIVERSITAT DE VALÈNCIA

CSIC
CONSEJO SUPERIOR DE INVESTIGACIONES CIENTÍFICAS

AITANA

IFIC INSTITUT DE FÍSICA CORPUSCULAR

IBIC 2026

15TH INTERNATIONAL BEAM INSTRUMENTATION CONFERENCE

Whistler Conference Centre

August 30th to September 3rd

Whistler BC, Canada

Thank you for your attention

This work has received financial support from the SO project CEX2023-001292-S funded byMICIU/AEI, the Plan Nacional PID2024-158190NB-C21, CDEIGENT 2021/012 and the ASFAE/2022/013, funded by the Generalitat Valenciana and the European Union's NextGenerationEU program. Additional support was provided by the European Union's Horizon Europe Marie Sklodowska-Curie Staff Exchanges program under grant agreement no. 101086276, and the MEXT (Development of key element technologies to improve the performance of future accelerators Program) Japan Grant Number JP-MXP1423812204.

laura.pedraza@ific.uv.es



Financiado por la Unión Europea NextGenerationEU

GOBIERNO DE ESPAÑA MINISTERIO DE CIENCIA, INNOVACIÓN Y UNIVERSIDADES

Plan de Recuperación, Transformación y Resiliencia

GENERALITAT VALENCIANA Conselleria de Educación, Universidades y Empleo

GVANEXT Fondos Next Generation en la Comunitat Valenciana

EAJADE Europe-America-Japan Accelerator Development Exchange Programme

EXCELENCIA SEVERO OCHOA

Backup-slides

A. Amplitude of the BPM modes

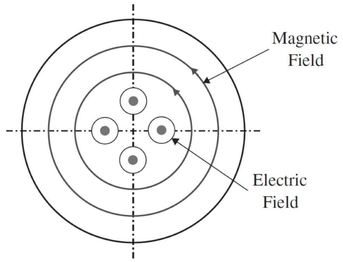
A) Pillbox cavity BPM

✦ **Resonant modes**

Field E_z:

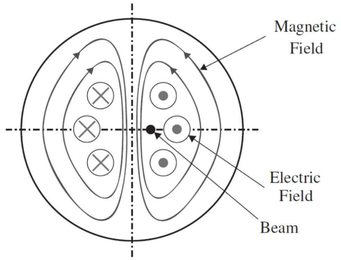
Monopole mode TM_{010}:

$$E_{z,010} = C_{010} J_0\left(\frac{j_{01} r}{a}\right) e^{i\omega_{010} t}$$



Dipole mode TM_{110}:

$$E_{z,110} = C_{110} J_1\left(\frac{j_{11} r}{a}\right) \cos\phi e^{i\omega_{110} t}$$



where C_{mnp} is the amplitude and $\omega_{mnp} = 2\pi f_{mnp}$ is the angular frequency of mode TM_{mnp}.

Resonance frequency of mode TM_{mnp} is:

$$f_{mnp} = \frac{c_0 k_{mnp}}{2\pi} \quad \text{where} \quad k_{mnp} = \sqrt{\left(\frac{j_{mn}}{a}\right)^2 + \left(\frac{p\pi}{L}\right)^2} \quad \Rightarrow \quad f_{010} = \frac{c_0 j_{01}}{2\pi a}, \quad f_{110} = \frac{c_0 j_{11}}{2\pi a}$$

where m, n, p are the node numbers, k_{mnp} is the wavenumber, a is the cavity radius, L is the length and j_{mn} is the nth zero of the mth Bessel function

- **(R/Q):** is defined as

$$\left[\frac{R}{Q_0}\right]_{mnp} = \frac{|\int \mathbf{E} d\mathbf{s}|^2}{P_{wall}} \frac{P_{wall}}{\omega_{mnp} W_s} = \frac{|V_{mnp}|^2}{\omega_{mnp} W_s}$$

  Used to evaluate the effect of the beam on the cavity and depends only on the cavity shape.

A. Amplitude of the BPM modes

A) Pillbox cavity BPM

- **Fundamental theorem of beam loading:**

"the voltage induced by a charge traveling through a cavity is twice the effective voltage "seen" by the charge itself"

Voltage of a mode in the cavity excited by the beam:

$$V_{b\to m} = q\frac{\omega_{mnp}}{2}\left(\frac{R}{Q}\right)_{mnp}$$

- **Output signal V_{out} :**

Stored energy in the cavity:

$$W_s = \frac{V_{b\to m}^2}{\omega_{mnp}(R/Q)_{mnp}} = q^2\frac{\omega_{mnp}}{4}\left(\frac{R}{Q}\right)_{mnp}$$

since $\left(\frac{R}{Q}\right)_{mnp} = \frac{|V_{mnp}|^2}{\omega_{mnp}W_s}$

By definition of Q_{ext}, the output power is:

$$P_{out} = \frac{\omega_{mnp}W_s}{Q_{ext}} = \frac{q^2\omega_{mnp}^2}{4}\frac{1}{Q_{ext}}\left(\frac{R}{Q}\right)_{mnp}$$

since $Q_{ext} = \frac{\omega_{mnp}W_s}{P_{out}}$

Output voltage (with impedance Z) is:

$$V_{out,0} = \sqrt{ZP_{out}} = \frac{q\omega_{mnp}}{2}\sqrt{\frac{Z}{Q_{ext}}\left(\frac{R}{Q}\right)_{mnp}}$$

A. Amplitude of the BPM modes

A) Pillbox cavity BPM

- **R/Q for each mode:**

Calculating $\left(\frac{R}{Q}\right)_{mnp} = \frac{|V_{mnp}|^2}{\omega_{mnp} W_s}$ using $V_{mn0}(\delta x) = \int_0^L E_{z,mn0}(r,\phi)\, \mathrm{d}z$ and $W_{s,mn0} = \int_V \frac{1}{2}\varepsilon_0 \left|E_{z,mn0}\right|^2 dV$

Dipole mode: $\left[\frac{R}{Q}\right]_{110} \propto J_1\left(\frac{j_{11} r}{a}\right)^2 \cos^2\phi \simeq \left(\frac{j_{11}\delta x}{a}\right)^2$

$\Rightarrow [R/Q]_{110} \propto (\delta x)^2$ for small offsets δx

Monopole mode: $\left[\frac{R}{Q}\right]_{010} \propto J_0\left(\frac{j_{01} r}{a}\right)^2 \simeq$ constante

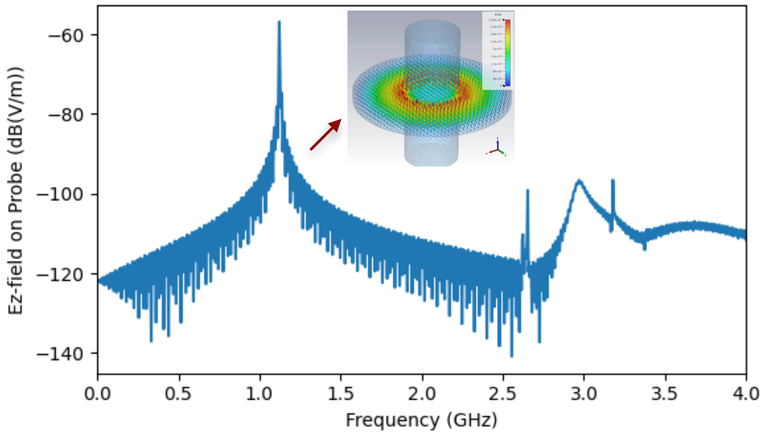
$\Rightarrow [R/Q]_{010} \propto$ constant

As $V_{out} \propto \sqrt{\left(\frac{R}{Q}\right)_{mnp}}$

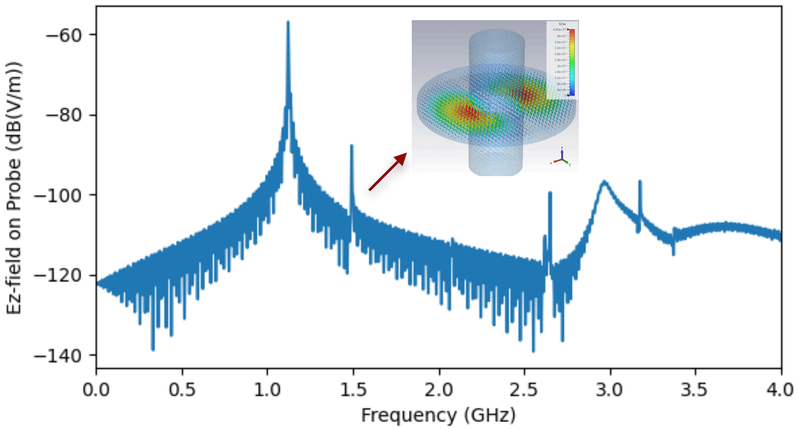
then $V_{out} \propto (\delta x)$ for the dipole

and $V_{out} \simeq$ constant for the monopole

- centered beam ($\delta x = 0$ mm)



- beam with offset ($\delta x = 0.5$ mm)



A. Amplitude of the BPM modes

A) Pillbox cavity BPM

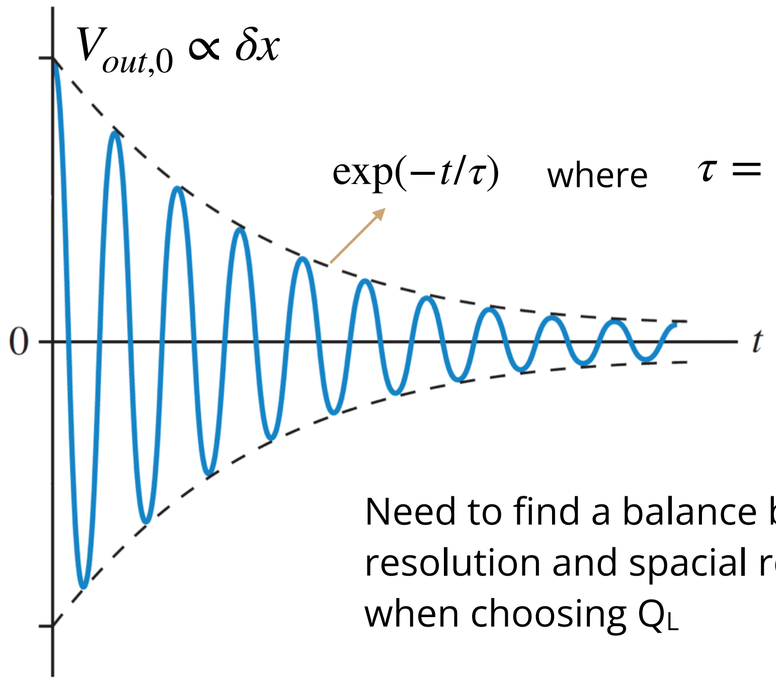
R. Lorenz, Cavity Beam Position Monitors, DESY
M. Viti, Resonant Cavities as Beam Position Monitor, DESY

➔ **Output signal**

❖ **on the time domain:**

The output signal oscillates at the dipole mode resonance frequency and decays exponentially with decay constant τ:

$$V_{out}(t) = V_{out,0}\sin(\omega_{mnp}t + \varphi)\exp(-t/\tau)$$



Need to find a balance between time resolution and spacial resolution when choosing Q_L

❖ **on the frequency domain:**

Contamination of the monopole signal at the dipole mode frequency

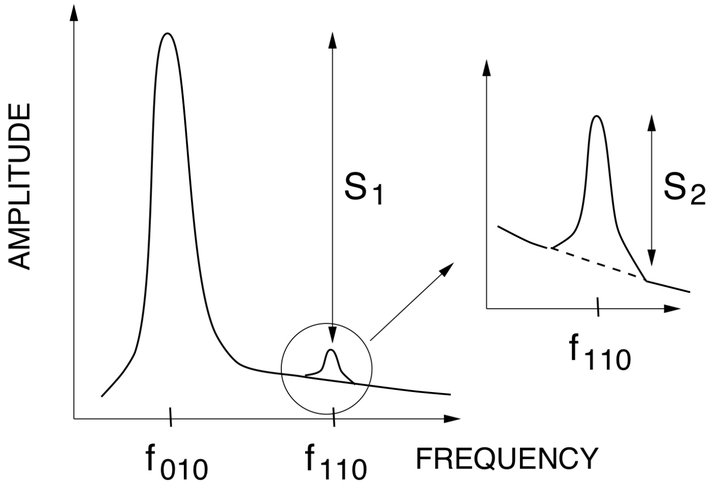


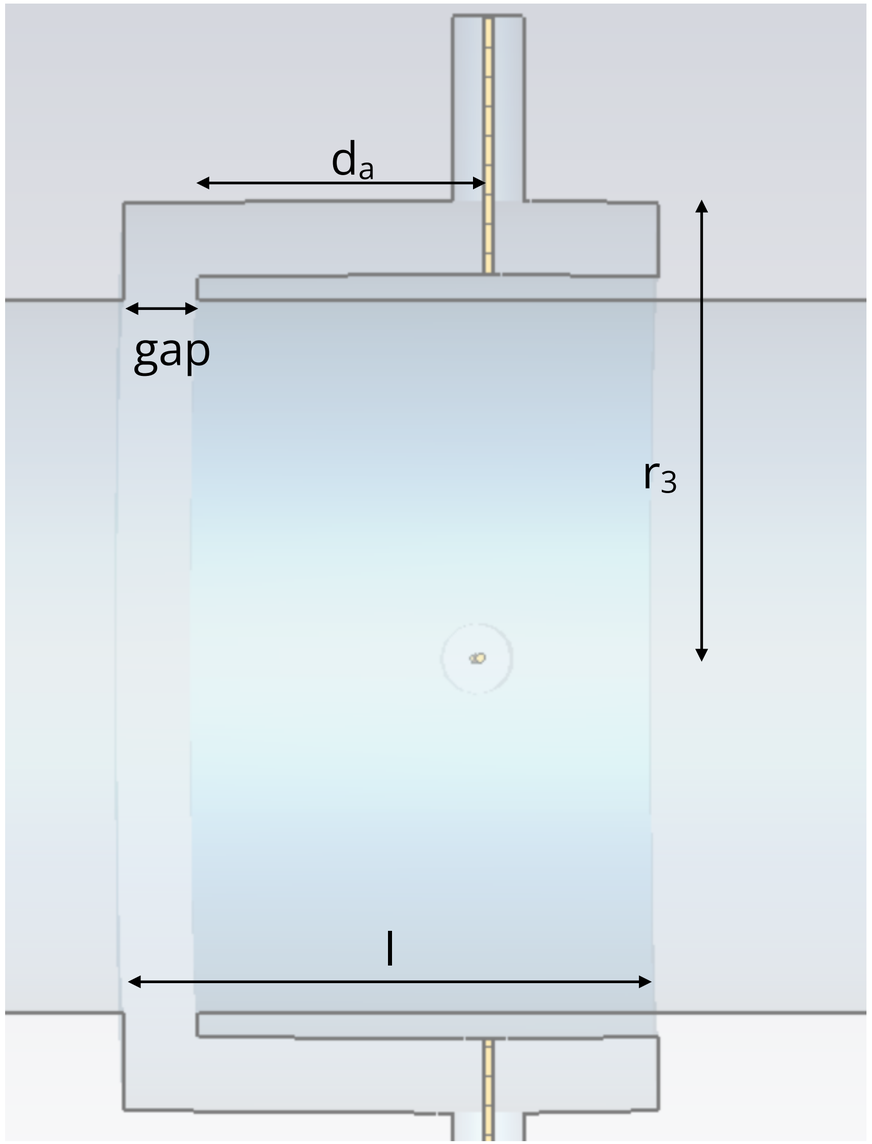
Figure: Common-mode contamination

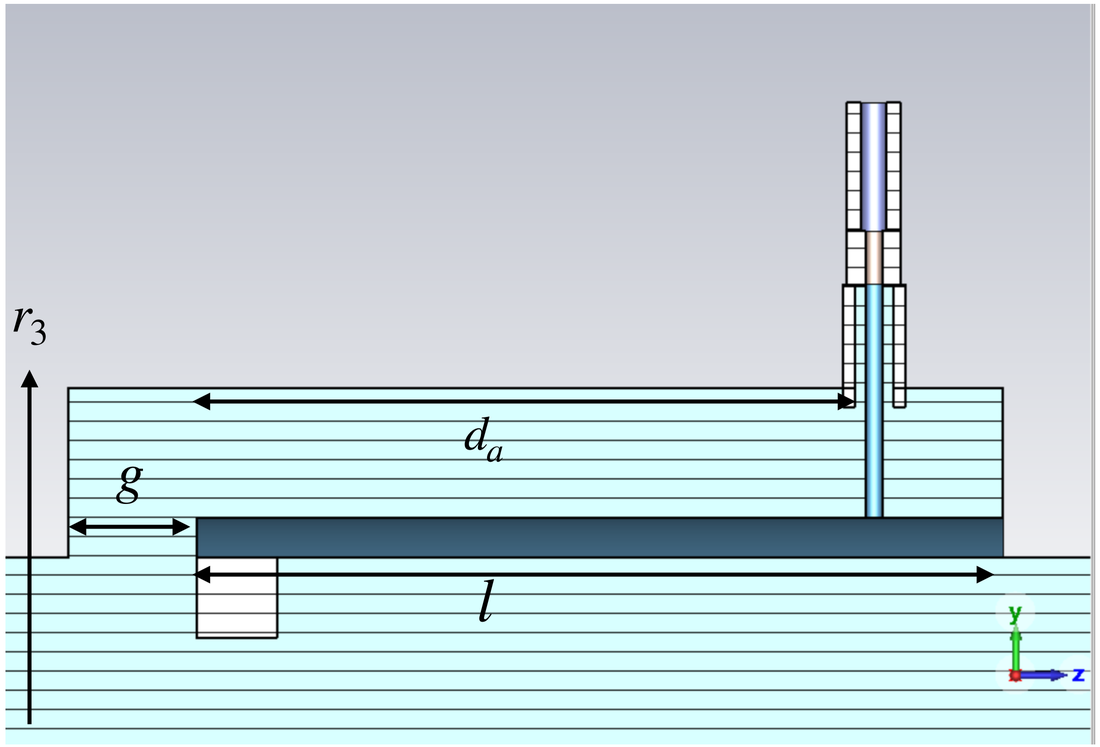
When recovering the dipole signal, there is the need to suppress the monopole mode (which is predominant).

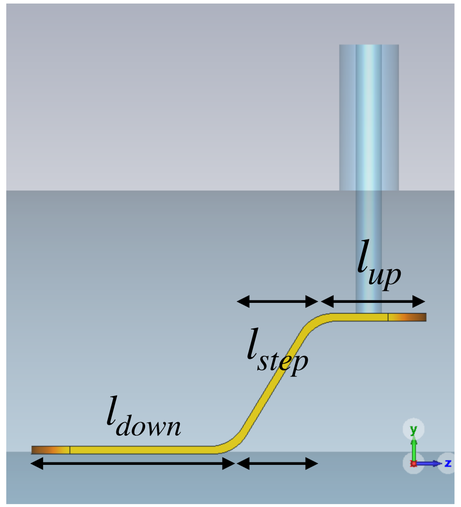
❖ **other considerations:**

- Aperture of the cBPM has to be similar to the aperture of the beam pipe

B. Parametric study

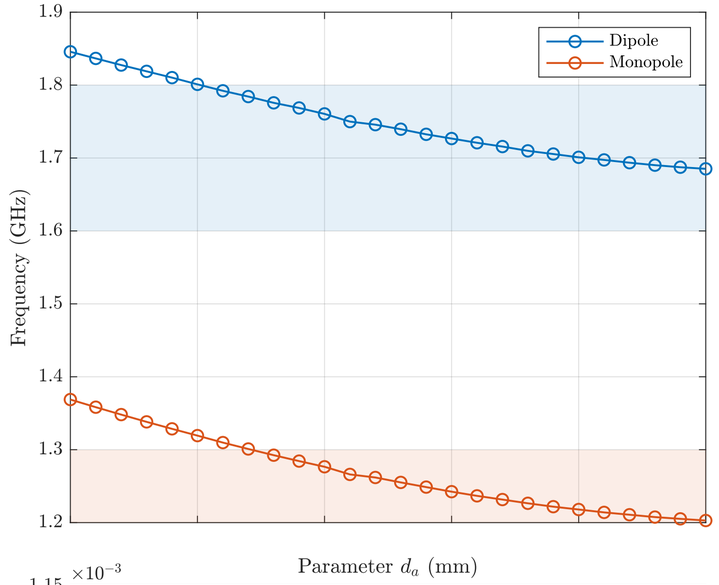


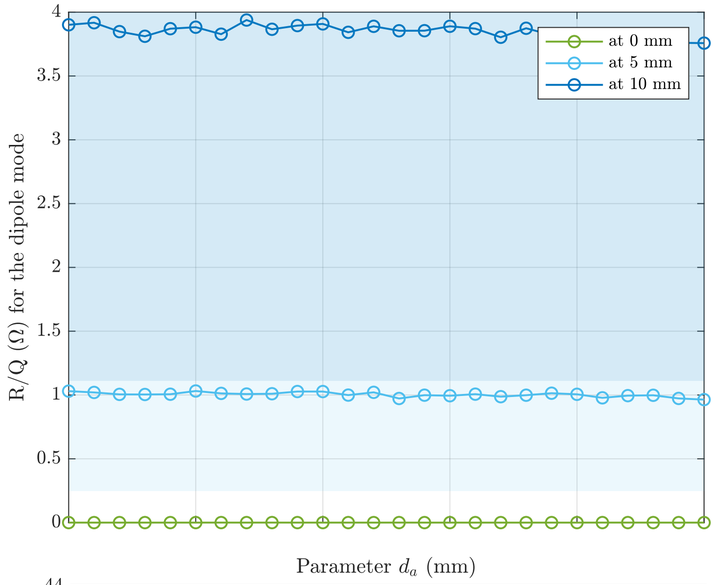


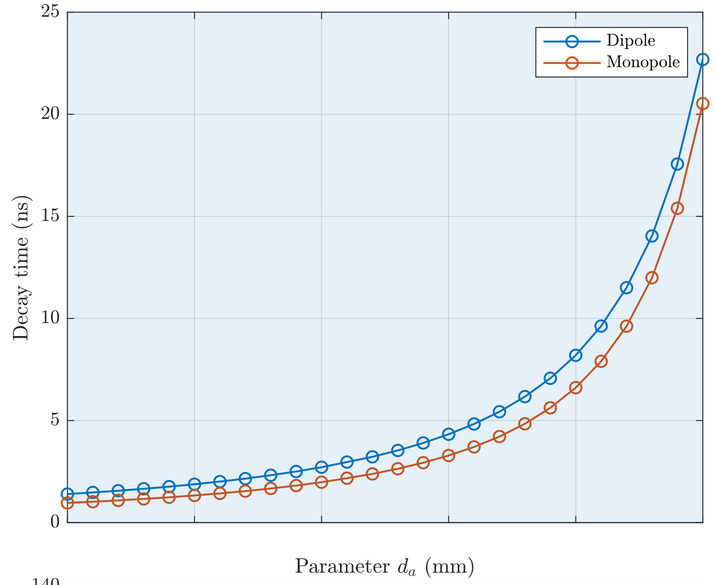


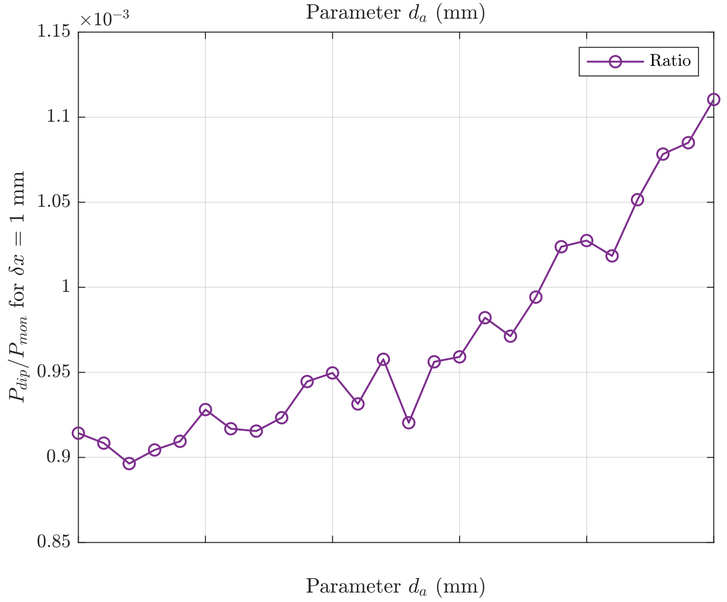
B. Parametric study

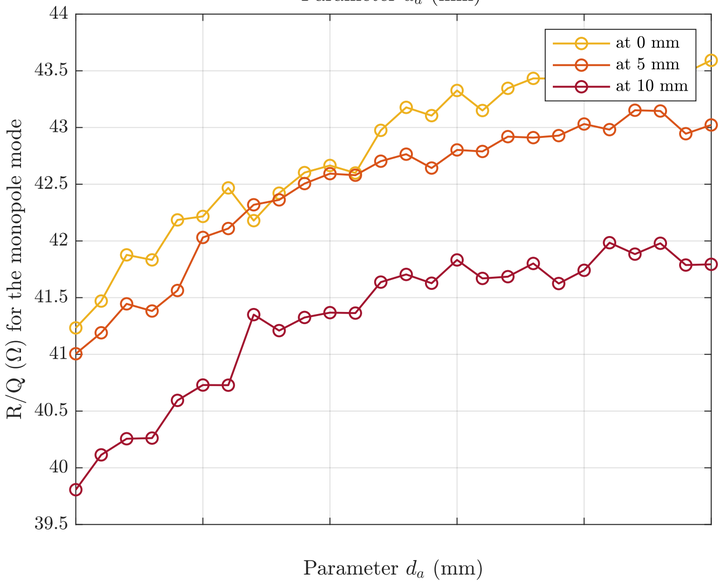
A) Antenna distance d_a

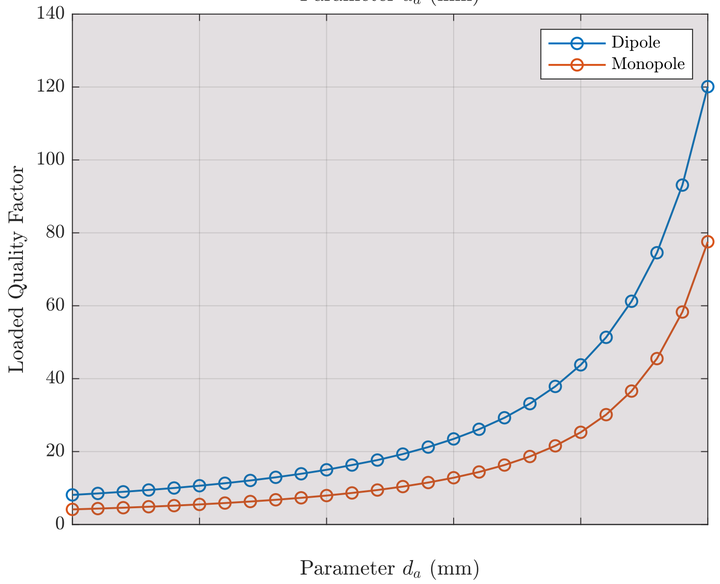






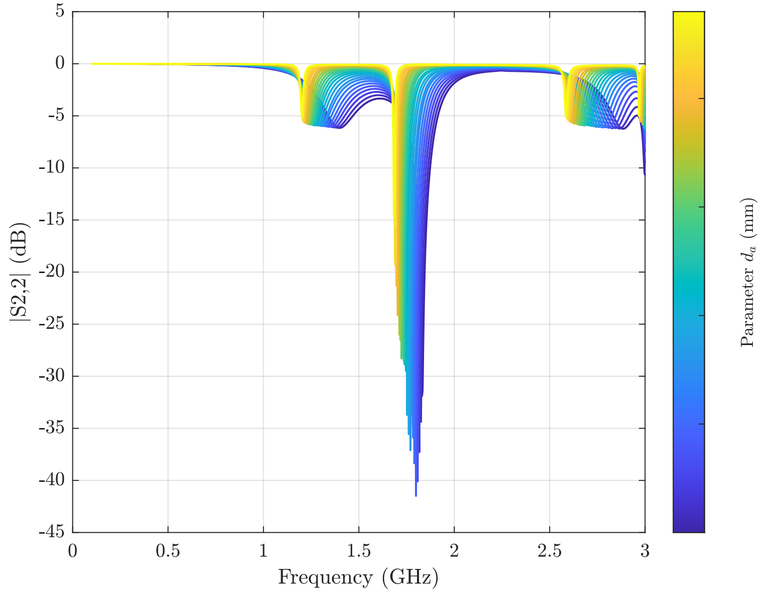


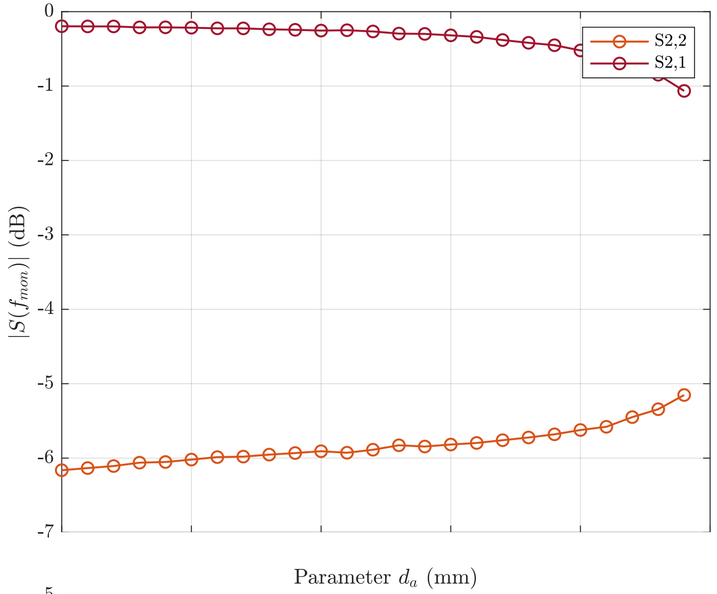


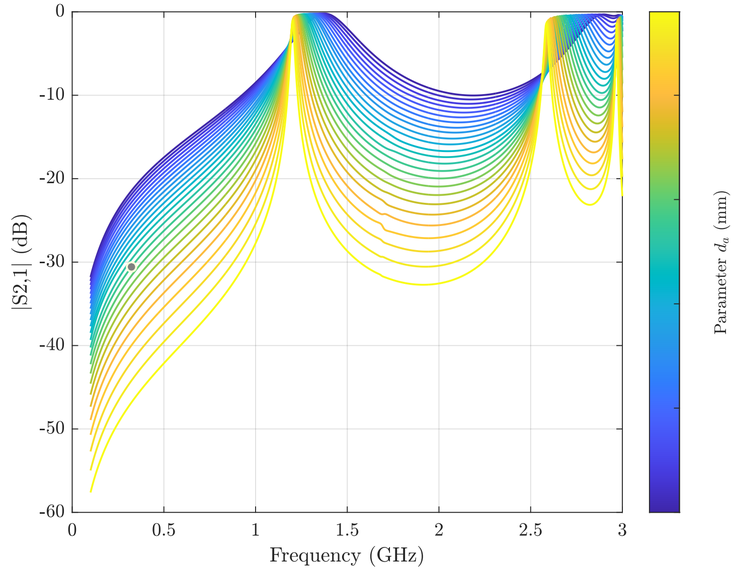


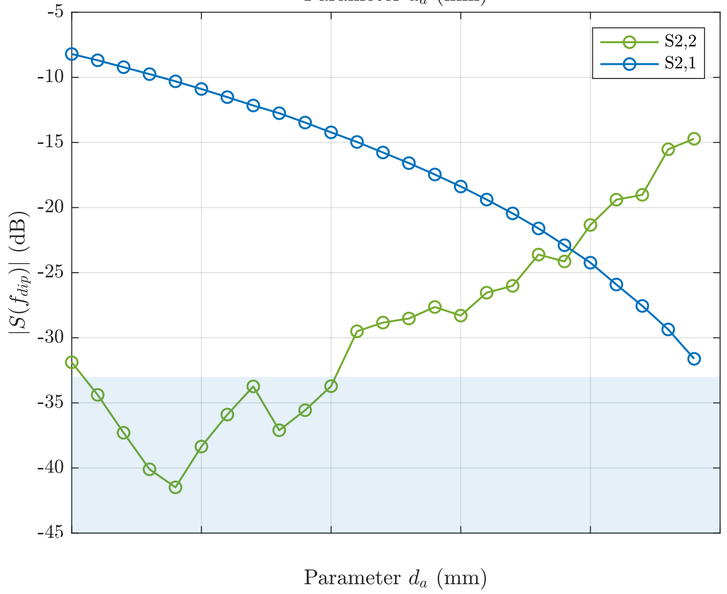
B. Parametric study

A) Antenna distance d_a







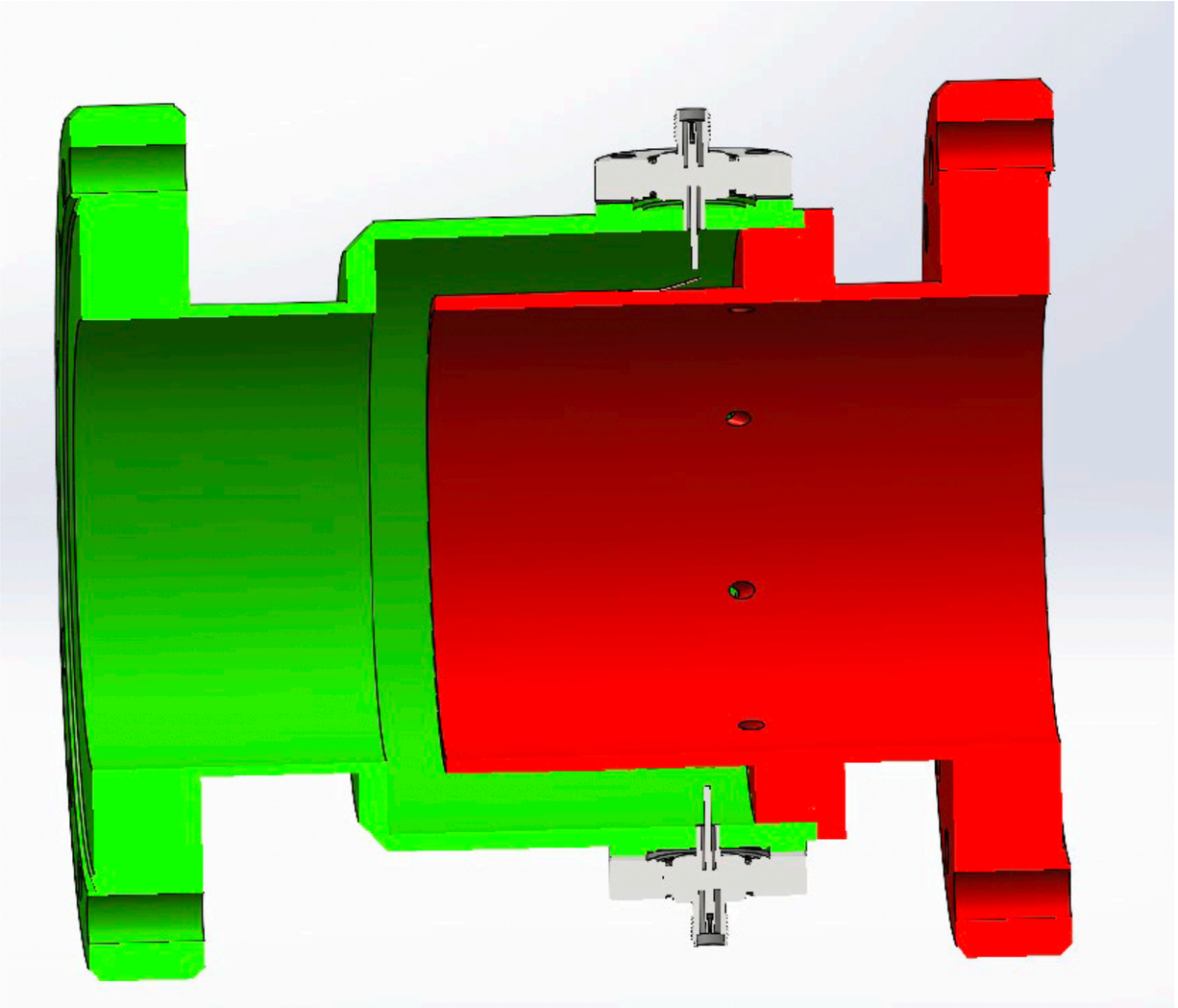


C. Commercial feedthrough

Conector coaxial: 15310-03-W (ri = 0.5 mm, ro = 1.1512 mm)

Length of the inner conductor of the antenna: 6,8 mm



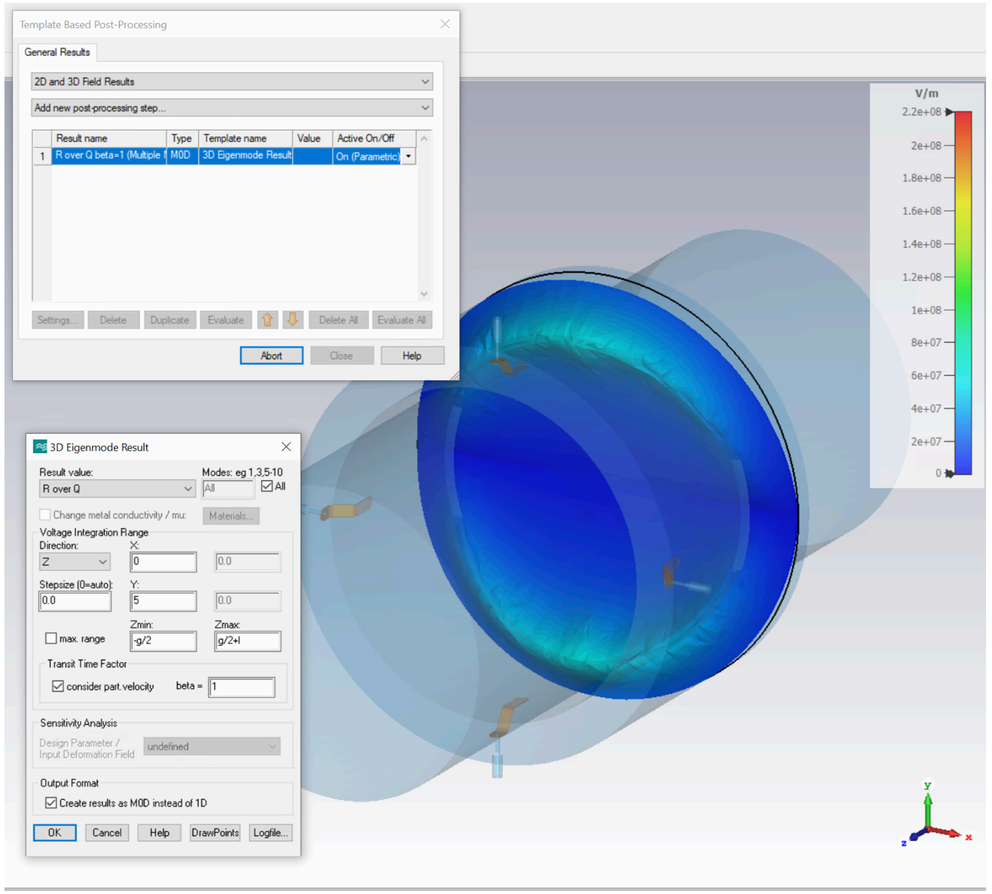


D. RF parameters calculation and measurements

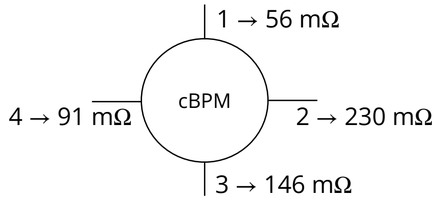
A) CST Studio suite

CST provides resonance frequencies and Q_L per mode.

Normalized Shunt Impedance simulation:

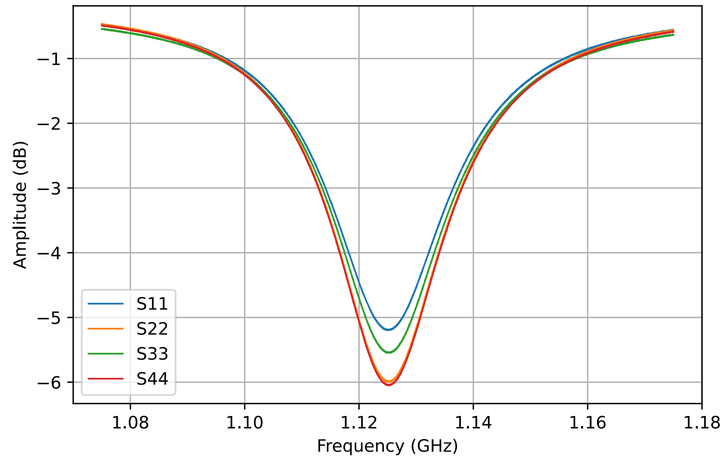


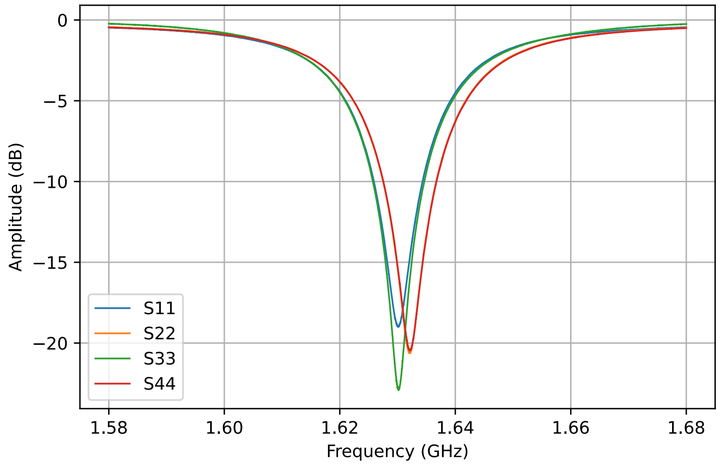
B) VNA Measurement



$$Q_L = \frac{f}{BW}$$

Step: 10 kHz





Averaging over all 4 ports:

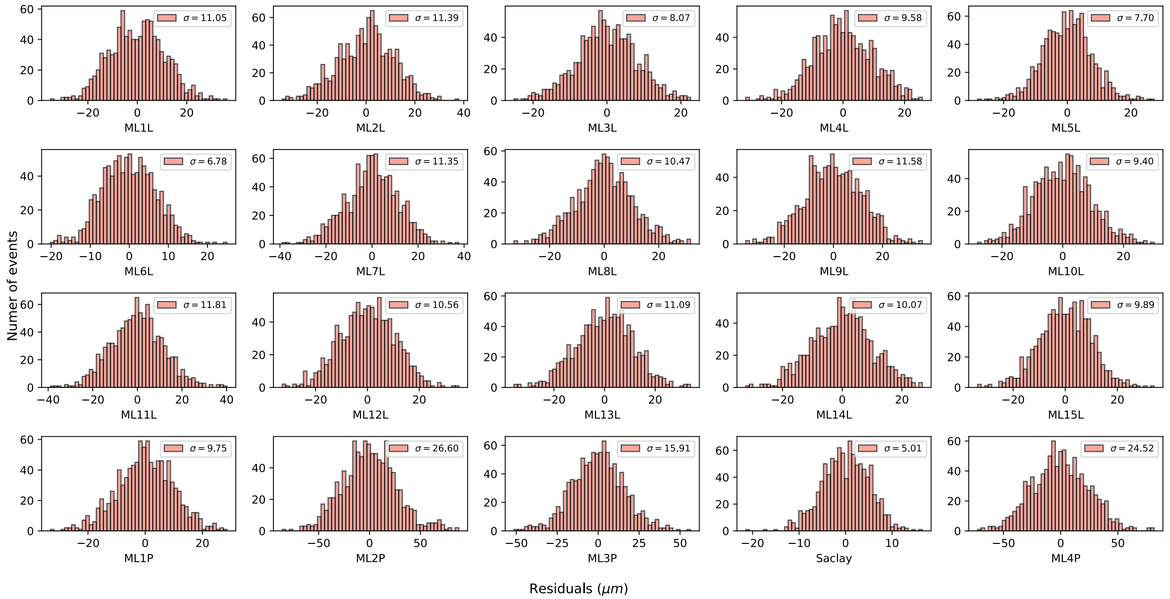
Loaded Quality factor		
	Monopole mode	**Dipole mode**
Minimum frequency	1.125 GHz	1.631 GHz
S-param at minimum	-5.70 dB	-20.76 dB
Band-width (at -3 dB)	24.0 MHz	28.2 MHz
Loaded quality factor	46.98	57.84

I. Summary of ATF measurements with BPM

A) Setup and methodology

Contribution of the resolution of other BPMs:

The previous method is employed for all BPMs:



Stripline BPMs showed resolutions between 7 μm and 25 μm, while the CEA-Saclay cBPM has shown to have a resolution of 3 μm under these beam conditions.

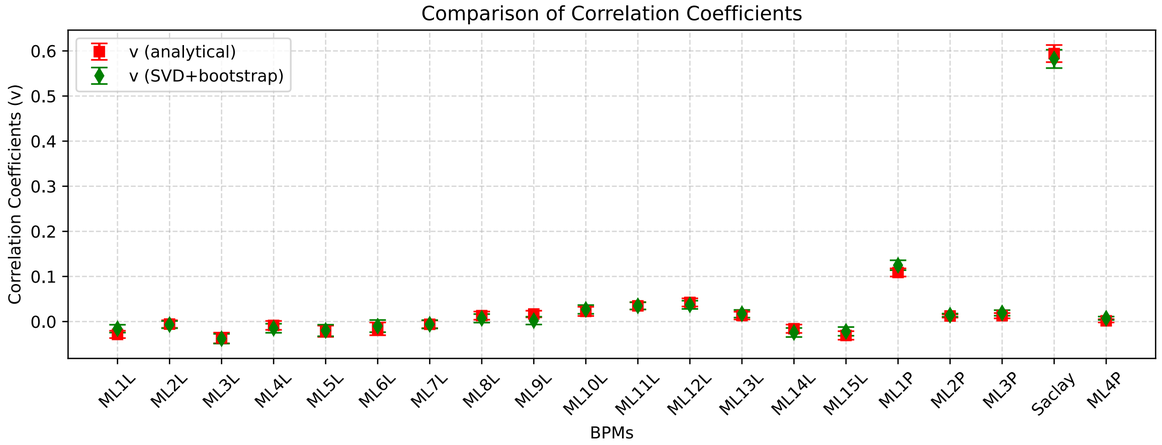
Uncertainties on the correlation coefficients from MIA:

- **Analytically:**
  from the square root of the diagonal elements of the covariance matrix $Cov(\mathbf{v})$, where

$$Cov(\mathbf{v}) = \sigma_{\hat{d}}^2 \left[\mathbf{D}^T\mathbf{D}\right]^{-1} = \frac{\| \mathbf{R} \|^2}{P-1} \left[\mathbf{D}^T\mathbf{D}\right]^{-1}$$

  assuming measurement noise in the cBPM is uncorrelated across pulses.

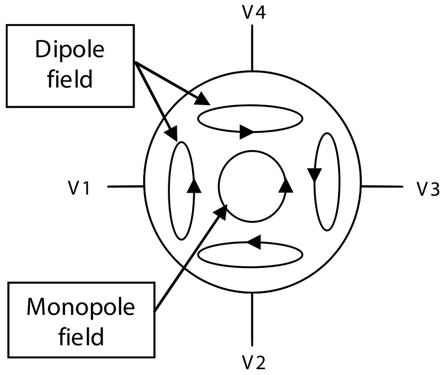
- **Via Bootstrap method:**
  resampling pulses from $\mathbf{d}$ and $\mathbf{D}$ with replacement and recalculating $\mathbf{v} = \mathbf{D}^{-1} \cdot \mathbf{d}$ [9]



E. Analog electronics specifics

A) 180º Hybrid and CM-rejection

Considering two opposing antennae, the TM010 field is the same and the TM110 field have a phase difference of π.

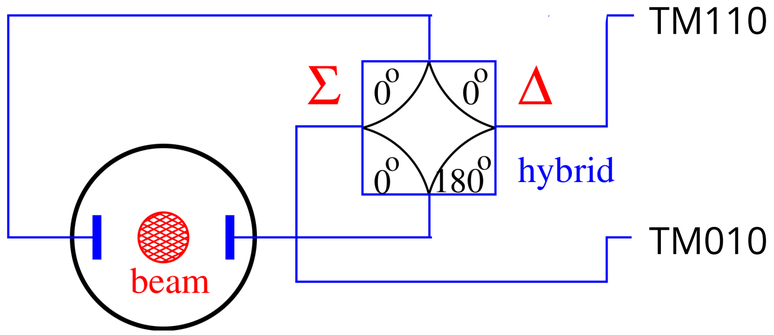


V1 = V(monopole) + V(dipole)
V2 = V(monopole) + V(dipole)
V3 = V(monopole) - V(dipole)
V4 = V(monopole) - V(dipole)

X = L (V1 - V3) / (V1 + V3)
Y = L (V2 – V4) / (V2 + V4)
L = constant

FIG. 2. (Color) Link between oscillation modes and beam position.

Use of a º180 hybrid to separate the modes:



The 'center resolution' is limited by the isolation between the Σ- and the Δ-ports of the device used

Then CM-rejection can be improved with: a **BPF** centered at the dipole frequency and **synchronous detection** of the dipole mode signal

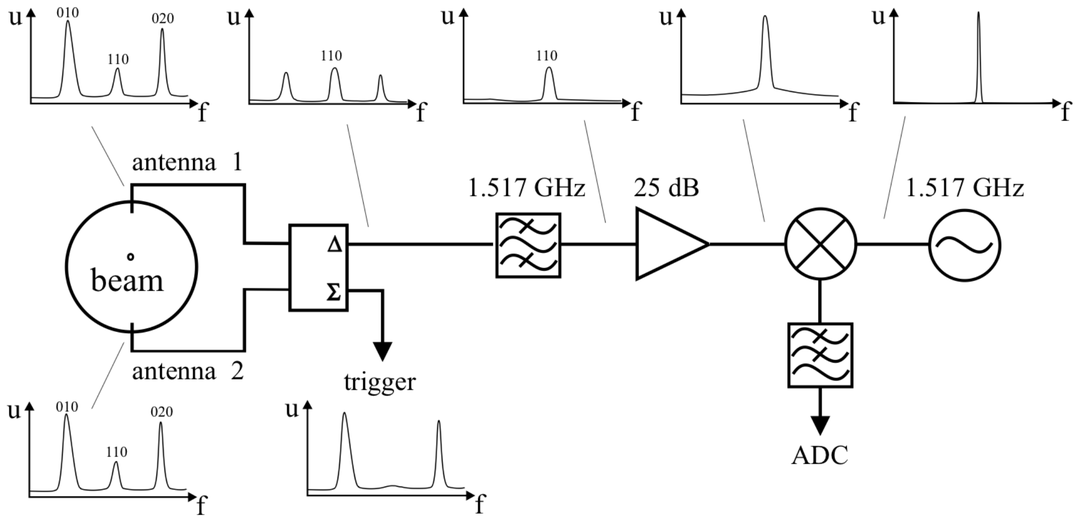
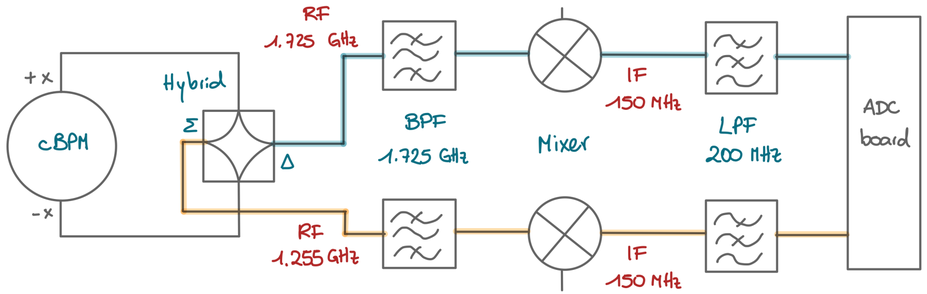


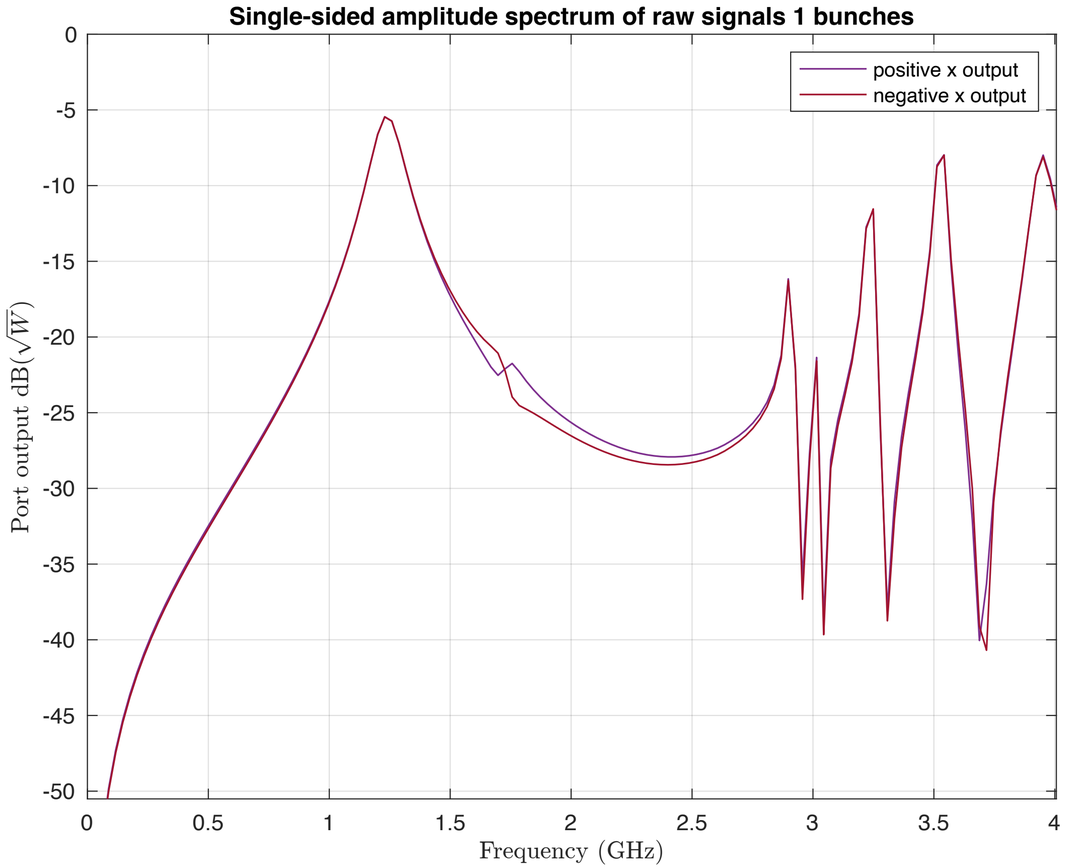
FIGURE 11. Block diagram of the homodyne receiver built for the detection of beam-excited vertical TM_{110} polarization (TTFL-monitors, Example 4). The mixer is realize an I/Q-mixer.

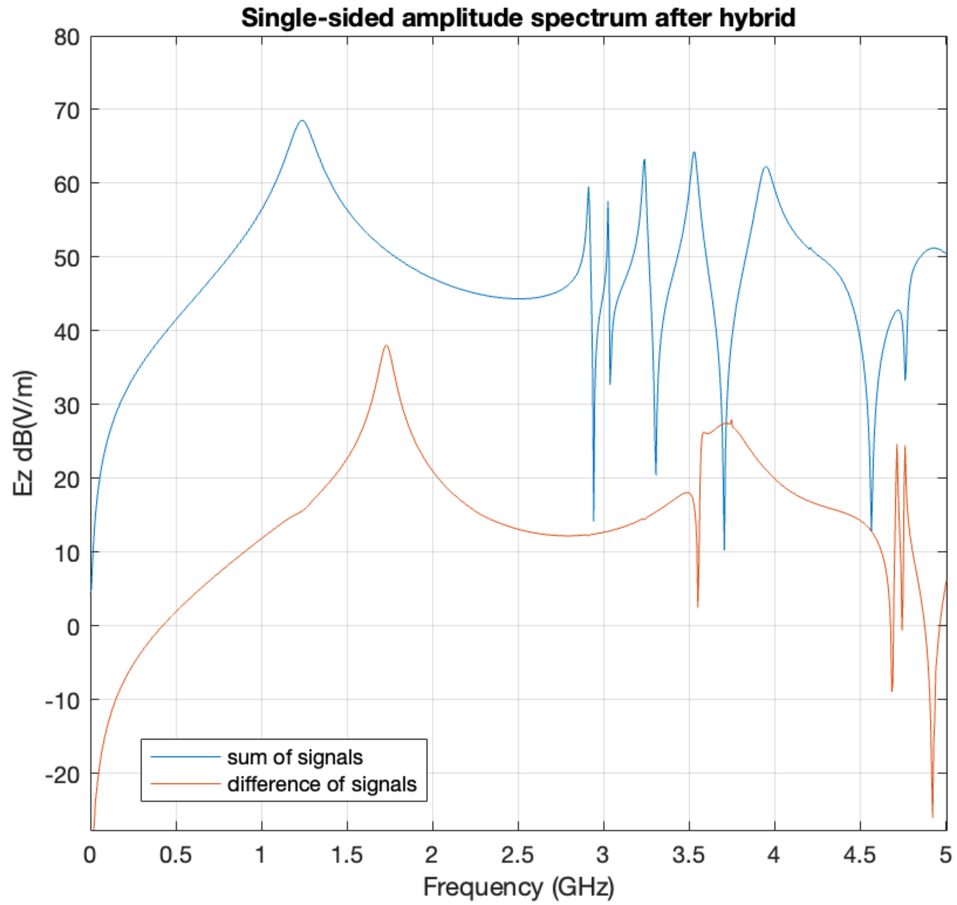
E. Analog electronics specifics

A) 180º Hybrid and CM-rejection

A simulation in CST+Matlab allows to evaluate the effect of the analog electronics components



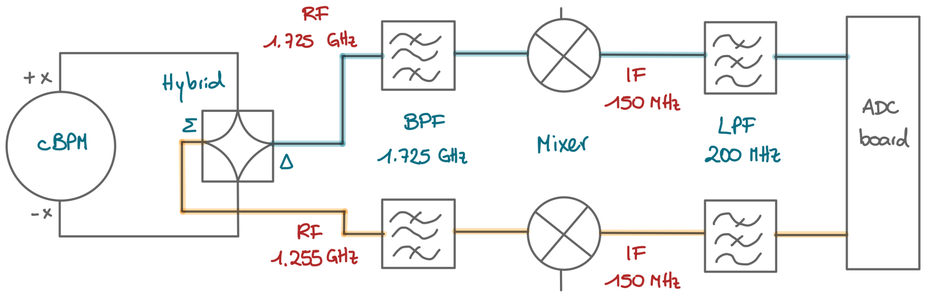




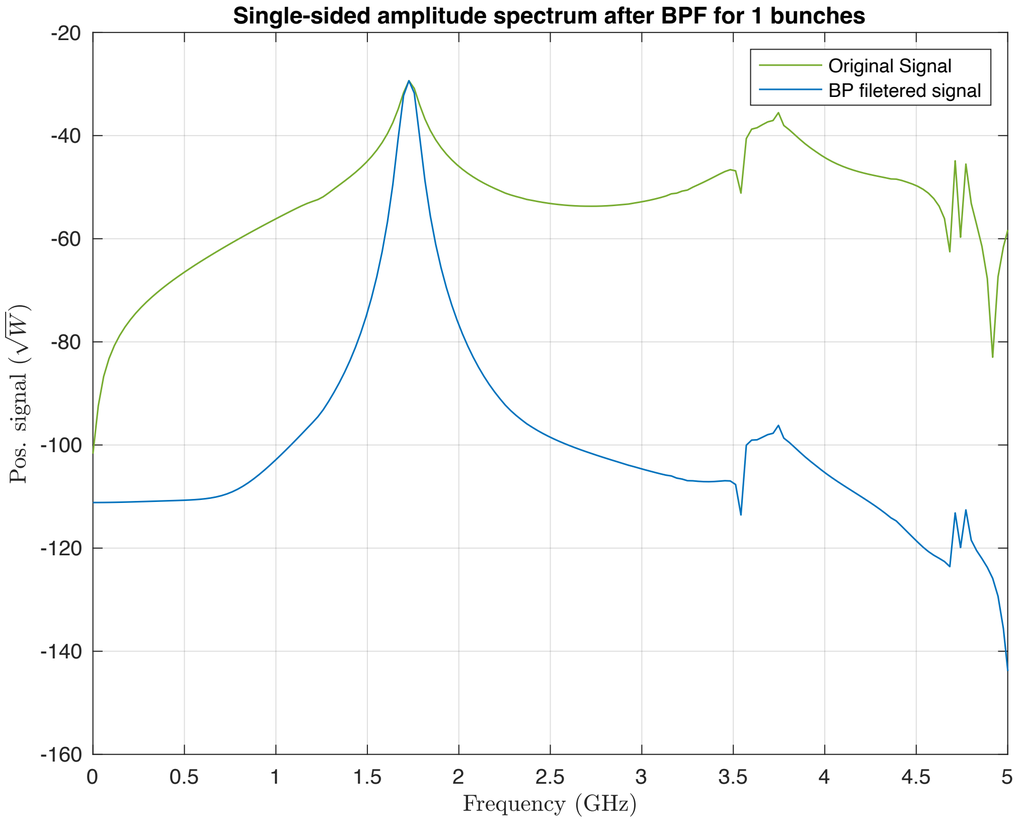
E. Analog electronics specifics

B) Filtering the tail of the monopole mode

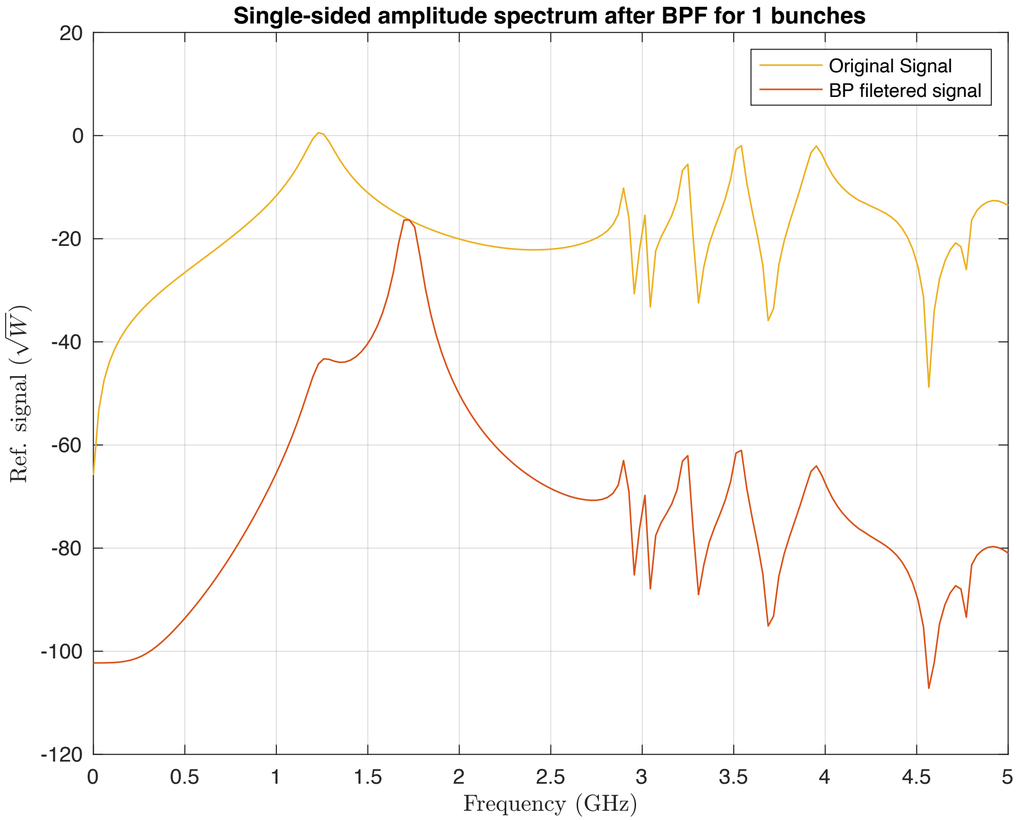
A simulation in CST+Matlab allows to evaluate the effect of the analog electronics components



For POSITION signal



For REFERENCE signal

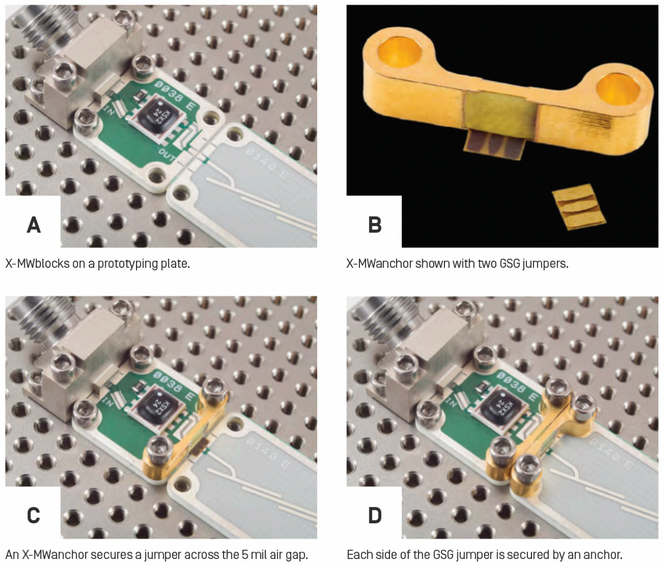


E. Analog electronics specifics

D) Quantic X-microwave modules

X-Microwave circuit modules:

- **planar transmission lines that are produced using photolithographic techniques**
- advantages:
  - ease of miniaturisation of microwave devices + production of simple two-layer boards
  - ease on design and prototyping + straightforward reconfiguration
  - excellent shielding and isolation when housing is employed → prevents external interference (Faraday cage)
  - relative low cost

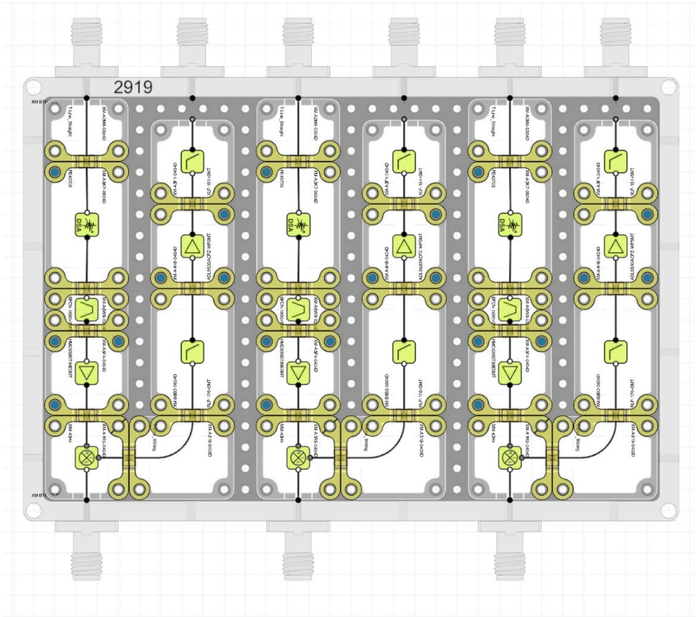


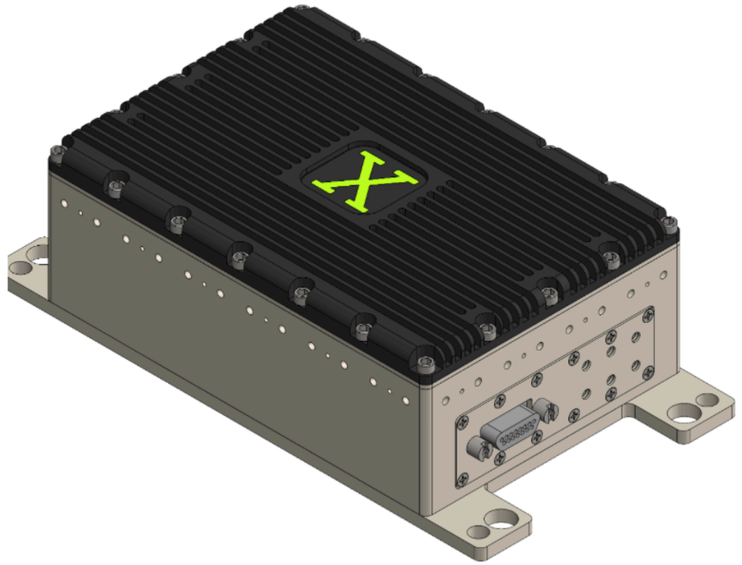
X-MWblocks on a prototyping plate.

X-MWanchor shown with two GSG jumpers.

An X-MWanchor secures a jumper across the 5 mil air gap.

Each side of the GSG jumper is secured by an anchor.





F. Digital Signal processing

A) DDC Algorithm

Algorithm for signal processing used commonly for cBPMs
The IF signals are demodulated digitally using a complex LO

- Signal captured by the digitiser at time t_j : $y_{dig}(t_j)$

- Down-converted filtered signal:

$$y_{DDC}(t_i) = \sum_{j=0}^{n\ samples} g(t_j - t_i)\exp\left[i\omega_{DDC}t_j\right] \cdot y_{dig}(t_j)$$

where $_i$ is the sample time

where ω_{DDC} is the angular frequency of the digital oscillator

where $_{g(t_i)}$ is a normalized Gaussian filter:

$$g(t_i) = \sqrt{2\pi}\sigma \exp\left[-\frac{t_i^2(2\pi\sigma)^2}{2}\right]$$

where σ is the filter bandwidth

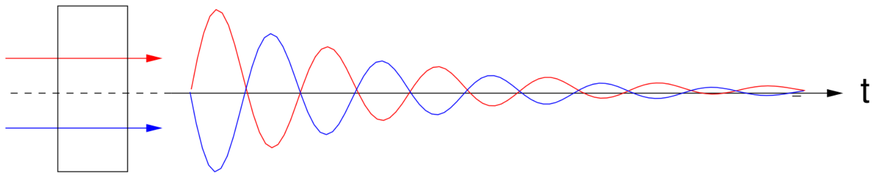
which is applied to remove noise and up-converted component of the signal

- Amplitude and phase of the demodulated signals:

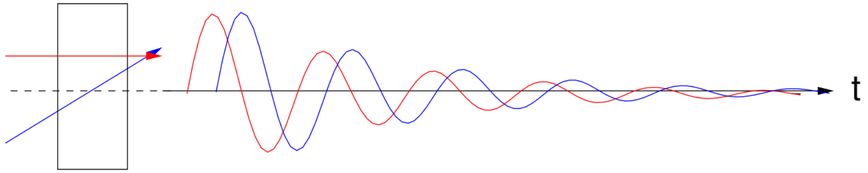
$$A(t_i) = \sqrt{y_{DDC}(t_i) \cdot y^*{}_{DDC}(t_i)} \quad \text{and} \quad \phi(t_i) = \arctan\left[\frac{\mathrm{Im}(y_{DDC}(t_i))}{\mathrm{Re}(y_{DDC}(t_i))}\right]$$

Procedure performed for position and reference signal independently

- Need of reference cavity to normalise charge $_q$ and noise produced by angle and tilt



(a) Same offset in opposite direction



(b) Position signal and angle signal

F. Digital Signal processing

A) DDC Algorithm

Signal cavity output: $V(t) = qe^{-t/\tau}e^{-i\omega t}(S_x\delta x + S_{x'}\delta x' e^{i\pi/2} + S_\theta \delta\theta e^{i\pi/2})$

where S_x, $S_{x'}$, S_θ are the cavity sensitivities to displacement, beam trajectory and bunch tilt.

- Beam position is calculated using in-phase $_I$ and quadrature-phase $_Q$ components of the demodulated signal

$$I = \frac{A_p(t_{DDC,d})}{A_r(t_{DDC,r})} \cos\left[\phi_p(t_{DDC,d}) - \phi_r(t_{DDC,r})\right]$$

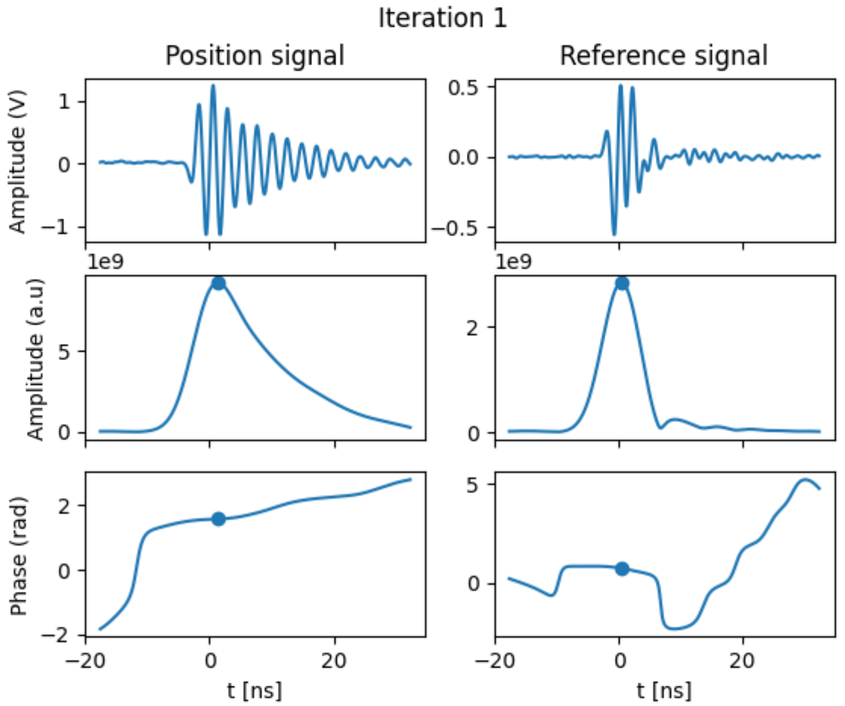
and

$$Q = \frac{A_p(t_{DDC,d})}{A_r(t_{DDC,r})} \sin\left[\phi_p(t_{DDC,d}) - \phi_r(t_{DDC,r})\right]$$

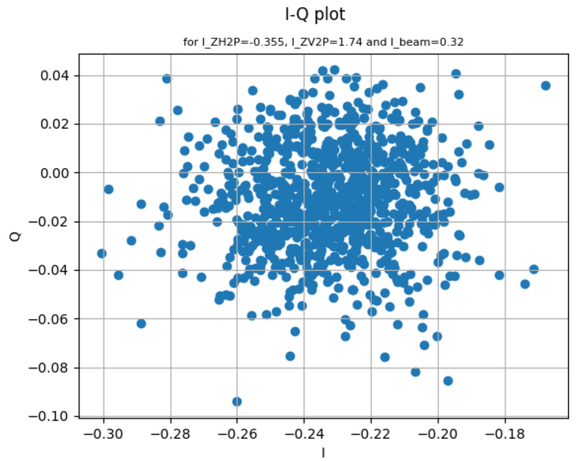
where $_p$ represents the position cavity and $_r$ represents the reference cavity.

- The sampling point $_{t_{DDC}}$ is selected to calculate $_I$ and $_Q$ at a certain time only.

Amplitude and phase reconstruction:



For a set of measurements for the same beam position:



F. Digital Signal processing

B) Calibration procedure

- **Determination of θ_{IQ}:**

  - I and Q are calibrated by shifting the beam position
  - Angle made with I axis is θ_{IQ}
  - Signal phasor (I, Q) is rotated to (P, T) by an angle of θ_{IQ}
  - Position dependence is only on the P direction
  - Angle and bunch tilt variation will be observed in T

$$P = I\cos\theta_{IQ} + Q\sin\theta_{IQ}$$

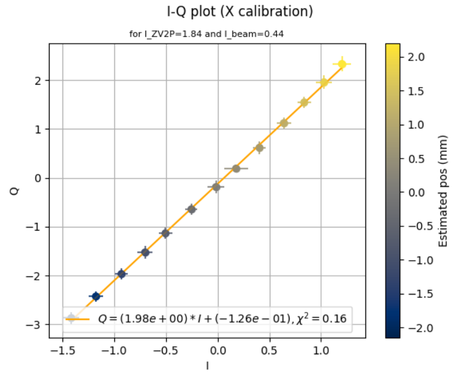
$$T = -I\sin\theta_{IQ} + Q\cos\theta_{IQ}$$

- **Determination of S_x:**
  - It is the relation between beam position and P

$$\delta x = S_x \cdot P\ (+a)$$

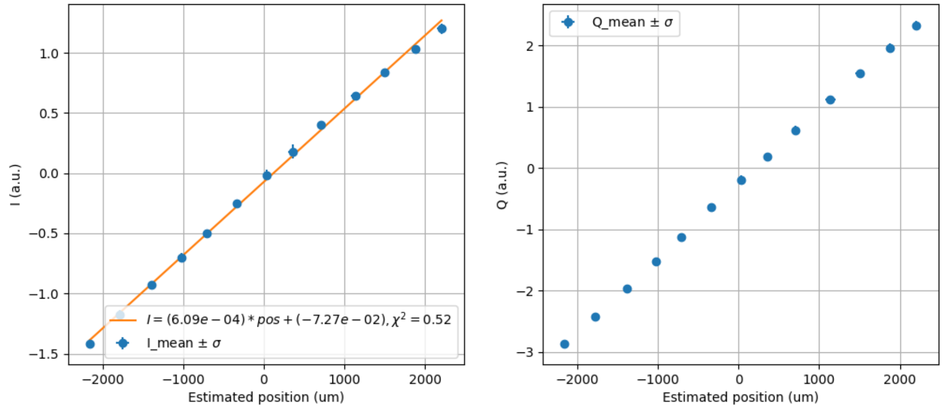
a is due to the misalignment between the BPM and the center of the pipe (or lack of calibration of striplines)

Signal phasor:



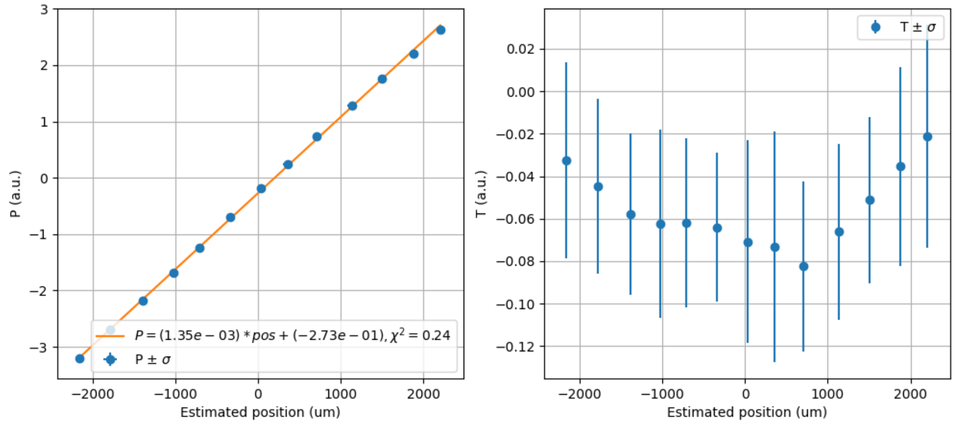
X calibration for I_ZV2P=1.84 and I_beam=0.44

Before rotation:



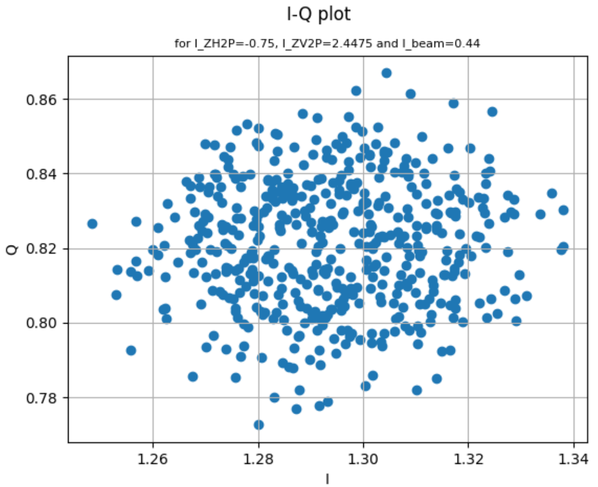
X calibration for I_ZV2P=1.84 and I_beam=0.44

After rotation:



G. Error calculation in Data processing

A) Error calculation for calibration procedure



For a single beam position, the mean value of the I and Q is taken, as well as the standard deviation σ.

```
I_mean = np.mean(I_values, axis = 1)
I_error = np.std(I_values, axis = 1)
```

Error calculation for θ_{IQ}, P and T: propagation of errors formula

$$\sigma_f = \sqrt{\left(\frac{\partial f}{\partial x}\right)^2 \sigma_x^2 + \left(\frac{\partial f}{\partial y}\right)^2 \sigma_y^2 + \left(\frac{\partial f}{\partial z}\right)^2 \sigma_z^2 + \cdots}$$

Error on the rotation angle:

$$\theta_{IQ} = \arctan(\alpha_{IQ}) \quad \Rightarrow \quad \sigma_\theta = \sqrt{\left(\frac{1}{1+\alpha^2}\right)^2 \sigma_\alpha^2}$$

where α_{IQ} is the slope of the IQ phasor and σ_α is its error

Error on the Position measure:

$$P = I\cos\theta + Q\sin\theta \quad \Rightarrow \quad \sigma_P = \sqrt{\cos\theta^2\sigma_I^2 + \sin\theta^2\sigma_Q^2 + (Q\cos\theta - I\sin\theta)^2\sigma_\theta^2}$$

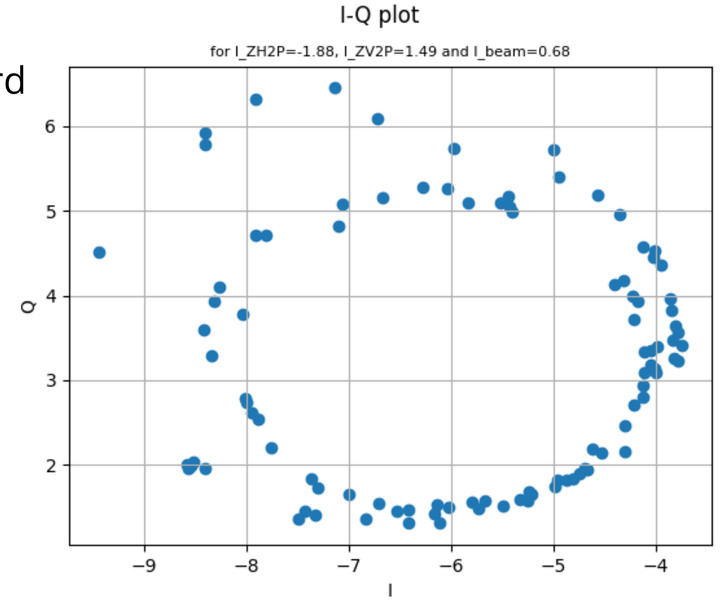
Error on the Tilt measure:

$$T = -I\sin\theta + Q\cos\theta \quad \Rightarrow \quad \sigma_T = \sqrt{\sin\theta^2\sigma_I^2 + \cos\theta^2\sigma_Q^2 + (-I\cos\theta - Q\sin\theta)^2\sigma_\theta^2}$$

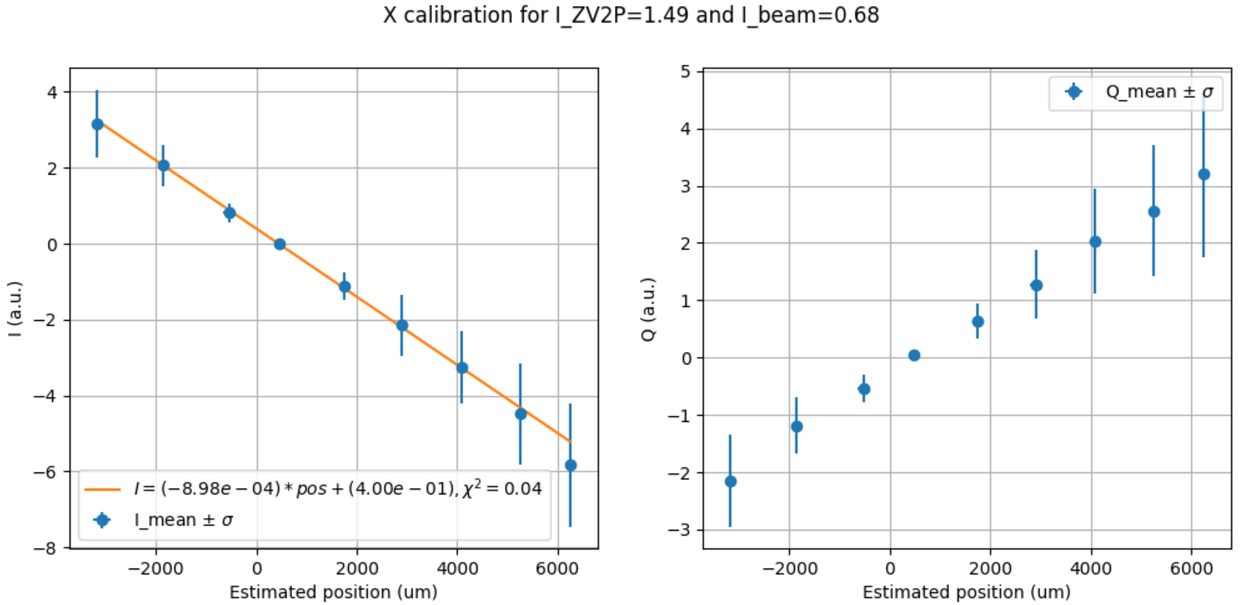
G. Error calculation in Data processing

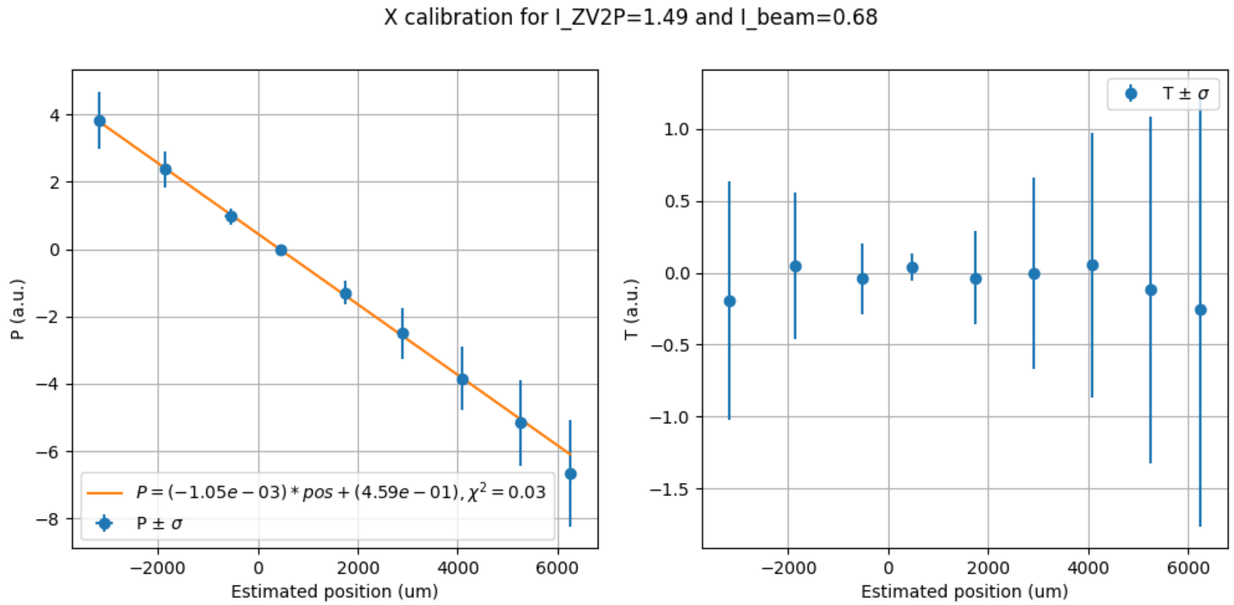
A) Error calculation for calibration procedure

Average and standard deviation of I and Q



Representation in plots:





Propagation of errors:

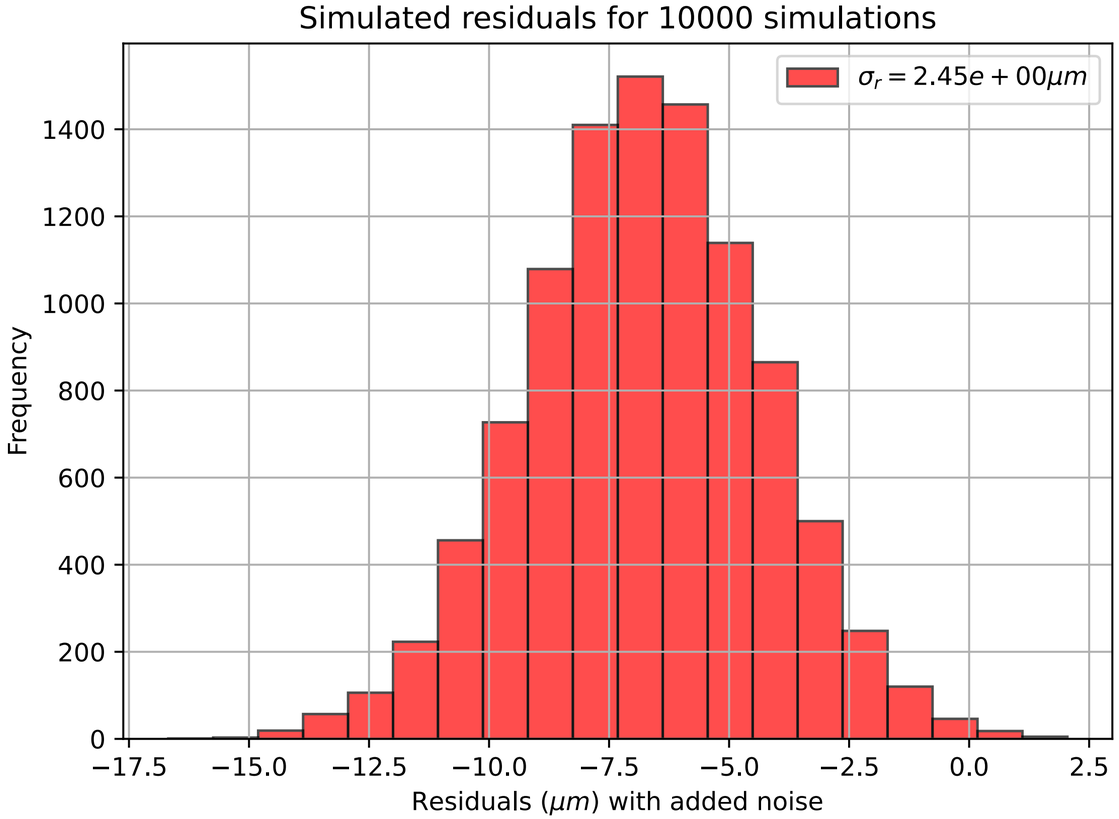
Representation in plots of **σ** to imply that ~68% of the data lies within the error bars.
Error bars illustrate the variability of measurements for each averaged point.

H. Resolution measurement limitations

A) Pseudo-experiments

INFLUENCE OF BPMs RESOLUTION AND CORRELATION COEFFICIENTS ERROR:

Pseudo-experiment considering $\sigma_{strip,i}$ and $\sigma(v_i)$ **only the last bunch**



Pseudo-experiment considering $\sigma_{strip,i}$ and $\sigma(v_i)$ **observing the stdv results over all bunches**

